Closed-form expression for the gravitational radiation rate from cosmic strings

Bruce Allen* and Paul Casper†

Department of Physics, University of Wisconsin-Milwaukee, P.O. Box 413, Milwaukee, Wisconsin 53201

(Received 15 March 1994)

We present a new formula for the rate at which cosmic strings lose energy into gravitational radiation, valid for all piecewise-linear loops of infinitely thin cosmic string. At any time, such a loop is composed of N straight segments, each of which has a constant velocity. Any cosmic string loop can be arbitrarily well approximated by a piecewise-linear loop with N sufficiently large. The formula is a sum of $O(N^4)$ polynomial and log terms, and is exact when the effects of gravitational back reaction are neglected. For a given loop, the large number of terms makes evaluation "by hand" impractical, but a computer or symbolic manipulator yields accurate results. The formula is more accurate and convenient than previous methods for finding the gravitational radiation rate, which require numerical evaluation of a four-dimensional integral for each term in an infinite sum. It also avoids the need to estimate the contribution from the tail of the infinite sum. The formula has been tested against all previously published radiation rates for different loop configurations. In the cases where discrepancies were found, they were due to numerical errors in the published work. We have isolated and corrected the errors in these cases. To assist future work in this area, a small catalog of results for some simple loop shapes is provided.

PACS number(s): 98.80.Cq, 04.30.Db, 11.27.+d

I. INTRODUCTION

Cosmic strings are one-dimensional topological defects which appear in some gauge theories of the fundamental interactions. Strings would appear at phase transitions where symmetries of the fundamental interactions are spontaneously broken [1–3]. It is thought that cosmic strings might have formed as the Universe expanded and cooled during the past. They are remarkably simple objects, characterized by a single parameter μ, which is their mass-per-unit length. For strings of cosmological interest, the expected value of the dimensionless parameter $G\mu/c^2$ is of order 10^{-6}, where G is Newton's gravitational constant and c is the speed of light. The strings of interest for this work are strings without ends—thus, they are always topologically in the form of circles, or possibly infinite in length (in a spatially infinite universe).

The dynamics of a network of cosmic strings in an expanding Universe have been thoroughly studied [4–6]. To describe these dynamics, it is useful to divide the strings, for the purposes of labeling, into two categories: the long string (length greater than the horizon length) and the loops (all the rest). Early work on cosmic strings established that the energy density of the long strings is a small constant fraction (of order $G\mu/c^2$) of the energy-density of the cosmological fluid. In the literature this is referred to as "scaling" behavior. The long string network maintains scaling behavior by constantly "chopping off" loops of cosmic string. This process takes place whenever long strings meet each other, make contact, and "intercommute." Typically, after a loop is chopped off it begins to oscillate due to its own tension, undergoing a process of self-intersection (fragmentation) and eventually creating a family of non-self-intersecting oscillating loops. In the absence of gravitational radiation, these loops would survive forever, oscillating periodically, and would eventually come to dominate the energy density of the Universe [1]. However, these loops gradually decay away due to the emission of gravitational radiation [3].

The emission of gravitational radiation is thus of fundamental importance to the topic of cosmic strings. Indeed, the resulting stochastic background of gravitational radiation left behind from the families of small string loops provides the main cosmological constraints on cosmic strings, through two observable effects [7 and references therein]. First, because gravitational radiation contributes to the energy-density, it affects the expansion rate of the Universe. The amount of gravitational radiation must not be too great or it would interfere with the highly successful standard model of nucleosynthesis. Second, the amount of gravitational radiation must not be too great to interfere with the extremely small timing residuals observed in the periods of a number of carefully observed fast pulsars. The work on these cosmological constraints is reviewed and updated in [7].

During the past 15 years a number of detailed calculations have been carried out to determine the rate at which cosmic string loops convert their energy into gravitational radiation. The power radiated by a given loop is

$$P=\frac{E}{\Delta t}=\gamma G\mu^2 c \ , \tag{1.1}$$

where E is the energy radiated in gravitational waves in a single oscillation of the loop, Δt is the period of that oscillation, and γ is a dimensionless constant that depends only on the shape of the loop and its velocity at any fixed instant in time. Thus the problem is to determine the numerical value of γ for a given string loop. Because loops

*Electronic address: ballen@dirac.phys.uwm.edu

†Electronic address: pcasper@dirac.phys.uwm.edu

are relativistic objects which have typical velocities of order c, the simplest approximation formulas such as the quadrupole approximation are not of much use, although in some cases they are reasonably accurate [8]. Vachaspati and Vilenkin [9] carried out the first detailed calculation of γ for a simple generalization of the circular loop. While some of the integrations were carried out analytically, the final integration over directions could only be done numerically. The next work was a hybrid analytic-numerical calculation by Burden [10] for a set of loops which were a variation of the Vachaspati and Vilenkin family. The first entirely exact analytic calculations were done by Garfinkle and Vachaspati [11] who considered a special family of "kinky" string trajectories. These are the simplest piecewise linear loops for which the exact formulas given in this paper may be applied directly. Additional work by Durrer [8] repeated some of the earlier calculations of the previous three groups and also investigated the accuracy of the quadrupole approximation for determining γ. The next work was a pair of papers by Scherrer, Quashnock, Spergel, and Press [12] and by Quashnock and Spergel [13], which developed numerical and analytic techniques to study the effects of gravitational back reaction on the shape and motion of the cosmic string loops. This is the first work which examines the way in which the shape of a string loop is changed as a result of the emission of gravitational radiation. (In our paper these effects are *not* taken into account—we assume periodic motion of the loop.) In addition to verifying some of Burden's results, they also obtained interesting results concerning the distribution of γ for typical families of non-self-intersecting string loops. Recent work by Allen and Shellard [14] used fast Fourier transform (FFT) methods to determine values of γ for the loops produced in their numerical simulation of cosmic string networks in an expanding Universe.

These investigations are important for the reason mentioned previously; the cosmological consequences of cosmic strings are largely visible via the direct and indirect effects of the gravitational waves produced by the string loops. Thus, "typical" or expected values of γ appear in expressions for observable quantities such as the present-day energy density expected in gravitational waves. Much of the research work on gravitational radiation by cosmic string loops has been motivated by a desire to determine the "typical" or "expected" values of γ. Thus, Scherrer, Quashnock, Spergel, and Press [12] give a histogram of the expected values of γ; the mean is $\gamma=61.7$ and the median is 55.4.

In much of the literature on this topic, the method used to determine γ is numerical. A loop of cosmic string radiates at discrete frequencies corresponding to the different normal modes of motion, so $\gamma=\sum_{n=1}^{\infty}\gamma_n$ is a sum of terms arising from each of these normal modes, labeled by $n=1,2,3,\ldots$. The value of each γ_n is given by an integral over the two-sphere of a particular function. This function, in turn, is a product of integral transforms over the world sheet of the loop. Except in certain highly symmetric cases, numerical methods must be used to determine the required four-dimensional integrals. Because it is only practical to determine γ_n up to n of a few hundred or thousand, one must extrapolate the dependence on n in order to estimate the "tail" terms arising in the infinite sum over n. This process is error prone because the sum over n may converge very slowly (if at all—with back reaction neglected, γ may be infinite). Also, if the integration over the two-sphere is not done accurately enough, the γ_n will be inaccurate for large n. This will cause the sum over n to converge at the wrong rate. Indeed, we have found that many of the previously determined values of γ given in the literature are incorrect (typically by a factor of order 2) because this tail has either not been included, or has been incorrectly estimated.

In this paper we develop a new method for determining γ. Our method yields an *exact analytic formula for* γ, valid for any piecewise linear cosmic string loop with piecewise linear velocity. (Equivalently, both the left- and right-moving trajectories are piecewise linear.) This piecewise linear requirement is really not very restrictive, since in practice any cosmic string loop can be *arbitrarily closely approximated* by a piecewise linear cosmic string. Thus *one can use this formula to determine* γ *to arbitrary precision for any cosmic string loop.* Remarkably, our formula involves nothing more complicated than logarithm and arctangent functions. However it is the sum of order N^4 terms, where N is the number of piecewise linear segments, and thus in practice is extremely cumbersome to evaluate without the assistance of a computer or symbolic manipulator. We stress that although our formula will probably never be evaluated without the use of a computer, it is *not a numerical method,* but rather is an *exact formula.* It is also fairly rapid—with N of 32 a DEC 3000 model 600 AXP Alpha workstation can evaluate γ in less than 2.5 sec. We are making our computer code, which provides one implementation of this algorithm, publicly available.[1]

In order to test our new formula we constructed piecewise linear approximations to the smooth cosmic string loops studied in earlier published calculations of γ. In a number of cases we obtained very close agreement between the value of γ given by our formula and the published values. However there were also a number of cases in which the results did not agree. Section VII contains further details of these cases. In every case where we had found disagreement we were able to show that our formula in fact had given the correct result. The disagreement in each case was due to numerical errors in the original work. Many of the published values of γ are off by about a factor of 2. For example, Vachaspati and Vilenkin give the value $\gamma=54.0$ for the case $\alpha=0.5$ and $\phi=0.5\pi$ in Eq. (2.24) of Ref. [9]. The correct value is $\gamma=97.2\pm2$. Note that the value of $\gamma=97.2$ is exact (to three significant figures) for the piecewise loop which we used to approximate the smooth Vachaspati and Vilenkin loop. The error bar of ±2 in γ arises because our piecewise approximation had only $N=64$ segments.

[1]Publicly available via anonymous FTP from the directory pub/pcasper at alpha1.csd.uwm.edu.

We intend to use this exact formula in future work, for example, to identify the shape of a cosmic string loop with the smallest value of γ, and to repeat some of the work of Scherrer, Quashnock, Spergel, and Press [12] concerning the distribution of γ values of non-self-intersecting loops.

The remainder of the paper is organized as follows. Section II describes the periodic motion of a cosmic string loop oscillating in flat space-time. It establishes notational conventions and a number of basic results. Note that in our approximation, the back reaction of gravity on the string loop is neglected, so that spacetime remains flat. In this context a given string loop oscillates periodically and radiates forever. Section III starts with a standard result [15] for the energy radiated by gravitational waves emitted from a periodic source, and obtains an integral representation for γ in terms of the gravitational interaction of the cosmic string world sheet with itself. This was motivated by (and is almost identical to) a calculation given in Appendix B of [13]. In Sec. IV we restrict our attention to the special case of piecewise linear loops, and establish notational conventions for such loops. The "corners" of the piecewise linear loop trajectory may be discretely labeled; their positions and velocities contain all information about the loop. The integral representation for γ is then expressed in terms of these discrete quantities. In Sec. V the formula for γ is simplified and expressed as a sum of elementary integrals. These integrals are three-dimensional volume integrals; the integrand is a Dirac δ function of a quadratic form in x, y, and z. These integrals are evaluated in closed form in Sec. VI. This section contains the main result of the paper, which is an exact closed-form expression for γ in the piecewise linear case. Section VII contains the results of our investigation of the existing literature, reporting both on those cases where we obtained agreement with published work, and those cases where we found the published work to be incorrect. In the latter cases, we have isolated the error(s) in the published work and report on how we corrected those errors. Section VIII contains a short "catalog" of values of γ for some elementary loop trajectories. This is followed by a short conclusion.

Note: throughout this paper we use the metric signature $(-,+,+,+)$, and denote Newton's constant by G. From here on we use units with the speed of light $c=1$.

II. COSMIC STRING MOTION IN FLAT SPACE

The trajectory of a cosmic string describes a two-dimensional world sheet in space-time. Points on the world sheet have space-time coordinates x^μ given by

$$x^\mu = x^\mu(\xi^0,\xi^1) \ , \tag{2.1}$$

where ξ^0 is a timelike and ξ^1 is a spacelike coordinate on the world sheet. The string is described by the Nambu action, which is proportional to the area of the world sheet:

$$S=-\mu\int[-g^{(2)}]^{1/2}d^2\xi \ . \tag{2.2}$$

Here μ is the mass-per-unit length of the string, $g^{(2)}$ is the determinant of the two-dimensional metric on the world sheet induced from the Minkowski metric, and the integration is over the entire world sheet of the string. If we define $x^\mu{}_{,a}=\partial x^\mu/\partial\xi^a$, where $a=0,1$, then the induced two-dimensional metric is given by

$$g^{(2)}_{ab}=g_{\mu\nu}x^\mu{}_{,a}x^\nu{}_{,b} \ . \tag{2.3}$$

If we denote time and space derivatives on the world sheet by an overdot$=\partial/\partial\xi^0$ and a prime$=\partial/\partial\xi^1$, then the determinant $g^{(2)}$ is

$$g^{(2)}=\dot{x}^\mu\dot{x}_\mu x'^\nu x'_\nu - x'^\mu\dot{x}_\mu\dot{x}^\nu x'_\nu \ . \tag{2.4}$$

Note that x'^μ is spacelike and $\dot{x}^\mu$ is timelike.

The Lagrangian equations of motion for the string are rather cumbersome [3]. However, the action (2.2) is invariant under the reparametrization (gauge transformation) $\xi^a\to\tilde{\xi}^a(\xi)$, so the equations can be simplified by a judicious choice of the parameters ξ^a. One may choose the parameters so that x^μ satisfies the gauge conditions

$$\dot{x}^\mu x'_\mu=0 \quad\text{and}\quad \dot{x}^\mu\dot{x}_\mu+x'^\mu x'_\mu=0 \ . \tag{2.5}$$

With this choice of gauge, the equation of motion is the two-dimensional wave equation

$$\ddot{x}^\mu-x''^\mu=0 \ . \tag{2.6}$$

The gauge conditions (2.5) still allow a further reparametrization where $\dot{\tilde{\xi}}{}^1=\tilde{\xi}'^0$ and $\tilde{\xi}'^1=\dot{\tilde{\xi}}{}^0$. Together these imply that $\ddot{\tilde{\xi}}{}^a=\tilde{\xi}''^a$. This allows us to set $\xi^0=t$. If we rename $\xi^1=\sigma$, then the coordinates of the string world sheet (2.1) become

$$x^\mu=x^\mu(t,\sigma) \ . \tag{2.7}$$

With this choice of parameters, the gauge conditions (2.5) become

$$\dot{x}^i x'_i=0 \quad\text{and}\quad \dot{x}^i\dot{x}_i+x'^i x'_i=1 \ , \tag{2.8}$$

where the index $i=1,2,3$ is a spatial index. The equation of motion becomes the two-dimensional wave equation

$$\ddot{x}^i-x''^i=0 \ . \tag{2.9}$$

The time part of the equation of motion (2.6) is satisfied automatically.

The general solution to the equation of motion (2.9) is

$$\mathbf{x}(\sigma,t)=\tfrac{1}{2}[\mathbf{a}(t+\sigma)+\mathbf{b}(t-\sigma)] \ . \tag{2.10}$$

Here, the function $\mathbf{a}$ defines the left-moving and $\mathbf{b}$ the right-moving component of the string. The first gauge condition applied to $\mathbf{x}$ implies that $\mathbf{a}'^2=\mathbf{b}'^2$, where here the prime means differentiation with respect to the function's argument. The second gauge condition implies that $\mathbf{a}'^2+\mathbf{b}'^2=2$. Together the gauge conditions force the functions $\mathbf{a}$ and $\mathbf{b}$ to satisfy

$$\mathbf{a}'^2=\mathbf{b}'^2=1 \ . \tag{2.11}$$

Up to this point, our treatment of cosmic strings includes both the case of infinite strings and the case of closed string loops. From here on, to study gravitational radiation, we consider only the case of closed loops. In this case, the world sheet of the (assumed non-self-intersecting) string has the topology of a cylinder $\mathbb{R}\times S^1$, and will be referred to as a "world tube." Because the string forms a closed loop, one finds an additional constraint on the otherwise arbitrary functions **a** and **b**.

If the cosmic string has the form of a closed loop, it follows that

$$\mathbf{x}(t,\sigma+L)=\mathbf{x}(t,\sigma) \quad \forall\sigma,t \;, \tag{2.12}$$

where the constant L is the length of the loop. This implies that

$$\mathbf{a}(t+\sigma)+\mathbf{b}(t-\sigma)=\mathbf{a}(t+\sigma+L)+\mathbf{b}(t-\sigma-L) \quad \forall\sigma,t \;. \tag{2.13}$$

If we define the null coordinates u and v by

$$u=t+\sigma, \quad v=t-\sigma \;, \tag{2.14}$$

then (2.13) becomes

$$\mathbf{a}(u+L)-\mathbf{a}(u)=\mathbf{b}(v)-\mathbf{b}(v-L) \quad \forall u,v \;. \tag{2.15}$$

However, because u and v can be varied independently, it must be the case that

$$\mathbf{a}(u+L)-\mathbf{a}(u)=\mathbf{b}(v)-\mathbf{b}(v-L)=\mathbf{c} \;, \tag{2.16}$$

where **c** is a constant vector. If we choose to work in the center-of-mass frame of the loop, then $\mathbf{c}=0$. This follows since in the center-of-mass frame we have

$$\begin{aligned} 0&=\int_0^L \dot{\mathbf{x}}\,d\sigma \\ &=\int_0^L \tfrac{1}{2}[\mathbf{a}'(t+\sigma)+\mathbf{b}'(t-\sigma)]d\sigma \\ &=\tfrac{1}{2}[\mathbf{a}(t+L)-\mathbf{b}(t-L)-\mathbf{a}(t)+\mathbf{b}(t)] \\ &=\mathbf{c} \;. \end{aligned} \tag{2.17}$$

Thus, in the center-of-mass frame, the functions **a** and **b** are periodic with period L:

$$\begin{aligned} \mathbf{a}(t+\sigma+L)&=\mathbf{a}(t+\sigma) \;, \\ \mathbf{b}(t-\sigma-L)&=\mathbf{b}(t-\sigma) \;. \end{aligned} \tag{2.18}$$

Because the functions **a** and **b** are periodic, each can be described by a closed loop. These loops will be referred to, respectively, as the a loop and the b loop. Together, the a and b loops define the trajectory of the string loop.

Because the functions **a** and **b** are periodic in their arguments, the string loop is periodic in time. The period of the loop is $L/2$ since

$$\begin{aligned} \mathbf{x}\left[t+\frac{L}{2},\sigma+\frac{L}{2}\right]&=\tfrac{1}{2}[\mathbf{a}(t+\sigma+L)+\mathbf{b}(t-\sigma)] \\ &=\tfrac{1}{2}[\mathbf{a}(t+\sigma)+\mathbf{b}(t-\sigma)] \\ &=\mathbf{x}(t,\sigma) \;. \end{aligned} \tag{2.19}$$

For the remainder of this paper we will set the loop length $L=1$. The period of the loop is then $\Delta t=L/2=\frac{1}{2}$, and the section of the world tube swept out by the loop in a single oscillation is covered by the coordinates $\sigma\in[0,1]$ and $t\in[0,\frac{1}{2}]$. The entire world tube is covered by $\sigma\in[0,1]$ and $t\in(-\infty,\infty)$.

The reason that one may set $L=1$ is remarkable: the power radiated in gravitational radiation from a loop of a given shape is invariant under a rescaling (magnification or shrinking) of the loop, provided that the velocity at each point on the rescaled loop is unchanged [3]. A formal proof of this is given in [14]. Thus, to calculate the radiated power it is sufficient to consider only those loops with total length $L=1$.

The null coordinates u and v defined in (2.14) are more convenient than the coordinates t and σ. The u,v coordinates are called null because the tangent four-vectors $\partial_u x^\alpha$ and $\partial_v x^\alpha$ associated with them are null. This follows because

$$\frac{\partial}{\partial u}=\frac{\partial\sigma}{\partial u}\frac{\partial}{\partial\sigma}+\frac{\partial t}{\partial u}\frac{\partial}{\partial t}=\frac{\partial}{\partial\sigma}+\frac{\partial}{\partial t}$$

and

$$\frac{\partial}{\partial v}=\frac{\partial\sigma}{\partial v}\frac{\partial}{\partial\sigma}+\frac{\partial t}{\partial v}\frac{\partial}{\partial t}=-\frac{\partial}{\partial\sigma}+\frac{\partial}{\partial t} \;, \tag{2.20}$$

are null vectors in Minkowski space. To be more explicit, since points on the world tube have space-time coordinates $[t,\mathbf{x}]$ given in terms of u and v by

$$x^\alpha(u,v)=\tfrac{1}{2}[u+v,\mathbf{a}(u)+\mathbf{b}(v)] \;, \tag{2.21}$$

the gauge conditions now imply that

$$\partial_u x^\alpha \partial_u x_\alpha=-(\tfrac{1}{2})^2+(\tfrac{1}{2})^2\mathbf{a}'^2=0$$

and

$$\partial_v x^\alpha \partial_v x_\alpha=-(\tfrac{1}{2})^2+(\tfrac{1}{2})^2\mathbf{b}'^2=0 \;. \tag{2.22}$$

Because of the periodicity of the loops, the world tube may be covered by the coordinates u and v in many equivalent ways. One convenient covering is to take $u\in[0,1]$ and $v\in(-\infty,\infty)$. The region of the world tube swept out in a single oscillation of the loop is then covered by $u\in[0,1]$ and $v\in[0,1]$. Note however that this is *not* the same region of the world-tube as $t\in[0,1/2]$ and $\sigma\in[0,1]$. This is shown in Fig. 1 of Ref. [14].

The energy-momentum tensor $T^{\mu\nu}$ for the string loop may be found by varying the action (2.2) with respect to the metric. In flat space, with our choice of coordinates and gauge, it is

$$T^{\mu\nu}(y^\alpha)=\mu\int_0^1 du\int_{-\infty}^{\infty} dv\, G^{\mu\nu}(u,v)\delta^4(y^\alpha-x^\alpha(u,v)) \;, \tag{2.23}$$

where $G^{\mu\nu}$ is defined by

$$G^{\mu\nu}(u,v)=\partial_u x^\mu\partial_v x^\nu+\partial_v x^\mu\partial_u x^\nu \;. \tag{2.24}$$

Note that the volume element for the (u,v) coordinates is related to that of the coordinates (t,σ) by the Jacobian of the coordinate transformation. Thus,

$$du\,dv=2\,d\sigma\,dt \;. \tag{2.25}$$

Because of the δ function which appears in (2.23), the stress tensor $T^{\mu\nu}$ vanishes everywhere except on the world sheet of the string loop.

III. POWER RADIATED IN GRAVITATIONAL RADIATION

The power emitted by an oscillating loop in the form of gravitational radiation may be determined in the weak-field limit. This is an excellent approximation for cosmologically interesting cosmic strings because the amplitude of the metric perturbation $h_{\mu\nu}$ is of order $G\mu/c^2 \approx 10^{-6}$. Because the gravitational radiation is weak, its back reaction on the loops does not modify a loop's motion significantly in a single oscillation. Hence we calculate the rate of gravitational radiation in the approximation that the back reaction can be neglected, so that a loop oscillates periodically in time.

The standard formulas used to calculate the power lost to gravitational radiation typically assume that the energy of the source is gradually dissipated into radiation, and that the stress-energy tensor of the source vanishes with time. In our case, the source is a periodically oscillating loop whose stress-energy tensor does not vanish with time, and therefore the standard formulas require minor modifications. Since the loops that we study in this paper have period $\frac{1}{2}$, they radiate only at discrete angular frequencies given by

$$\omega_n = 4\pi n \quad \text{for } n = 1,2,3,\ldots . \tag{3.1}$$

The power radiated per unit solid angle into the nth mode is given by the standard formula (Eq. 10.4.13 of [15])

$$\frac{dP_n}{d\Omega} = \frac{G}{\pi}\omega_n^2[\tau^*_{\mu\nu}(\omega_n\Omega)\tau^{\mu\nu}(\omega_n\Omega) - \tfrac{1}{2}|\tau^\lambda{}_\lambda(\omega_n\Omega)|^2] . \tag{3.2}$$

In this equation, the Fourier transform of the stress-energy tensor is defined by

$$\tau_{\mu\nu}(\omega\Omega) \equiv \lim_{T\to\infty}\frac{1}{2T}\int_{-T}^{T}dt\int d^3x\, e^{i\omega(t-\Omega\cdot\mathbf{x})}T_{\mu\nu}(t,\mathbf{x}) , \tag{3.3}$$

and an asterisk denotes complex conjugation. The vector $\mathbf{x}$ is an ordinary flat-space three-vector, and Ω is a unit length three-vector with spatial Cartesian components given by

$$\Omega = (\cos\phi\sin\theta, \sin\phi\sin\theta, \cos\theta) . \tag{3.4}$$

To calculate the total radiated power, one must integrate over all directions on the unit sphere. This introduces integrals of the form

$$\int d\Omega\, f(\Omega) \equiv \int_0^\pi \sin\theta\, d\theta\int_0^{2\pi}d\phi\, f(\theta,\phi) \tag{3.5}$$

into the equations that follow.

The Fourier transform of the stress-energy tensor (3.3) is defined as the limit of a infinite-time integral. This differs slightly from the case of nonperiodic sources. It is easy to see that $\tau_{\mu\nu}(\omega\Omega)$ vanishes unless ω takes on one of the discrete values ω_n. [This is shown in Ref. [14] following Eq. (3.11).] For these values of ω_n, the $T\to\infty$ limit of the integral is not hard to calculate: since the source is periodic, the limit appearing in (3.3) is equal to the integral over a single period, i.e., the same integral with $2T$ set equal to $\frac{1}{2}$. Substituting expression (2.23) for the stress-energy tensor into the formula for $\tau_{\mu\nu}$ one finds that

$$\tau_{\mu\nu}(\omega_n\Omega) = 2\mu\int_0^1 du\int_0^1 dv\, G_{\mu\nu}(u,v)\exp(i\omega_n\{u+v-\Omega\cdot[\mathbf{a}(u)+\mathbf{b}(v)]\}/2) . \tag{3.6}$$

Note that the limits of integration in (u,v) space cover one complete oscillation period of the world sheet of the string loop.

The total radiated power is obtained by summing over all the modes:

$$P = \sum_{n=0}^{\infty}\int d\Omega\frac{dP_n}{d\Omega} . \tag{3.7}$$

The $n=0$ mode has been included in the sum for later convenience; it makes no contribution because of the factor of ω_n^2 appearing in (3.2). This expression for the total power can be put into a more useful form by using the explicit formula (3.6) for the Fourier transform of the stress tensor. This gives

$$P = \frac{2G\mu^2}{\pi}\sum_{n=-\infty}^{\infty}\omega_n^2\int d\Omega\int_0^1 du\int_0^1 dv\int_0^1 d\tilde{u}\int_0^1 d\tilde{v}\, \psi(u,v,\tilde{u},\tilde{v})\exp\{i\omega_n[\Delta t(u,v,\tilde{u},\tilde{v}) - \Omega\cdot\Delta\mathbf{x}(u,v,\tilde{u},\tilde{v})]\} , \tag{3.8}$$

where we have defined

$$\psi(u,v,\tilde{u},\tilde{v}) = G_{\mu\nu}(u,v)G^{\mu\nu}(\tilde{u},\tilde{v}) - \tfrac{1}{2}G^\lambda{}_\lambda(u,v)G^\gamma{}_\gamma(\tilde{u},\tilde{v}) . \tag{3.9}$$

The functions $\Delta t = (u+v-\tilde{u}-\tilde{v})/2$ and $\Delta\mathbf{x} = [\mathbf{a}(u)+\mathbf{b}(v)-\mathbf{a}(\tilde{u})-\mathbf{b}(\tilde{v})]/2$ in (3.8) describe the temporal and spatial separation of the two points on the string world sheet with coordinates (u,v) and $(\tilde{u},\tilde{v})$, respectively. To save space, in some of the formulas that follow, the arguments of Δt and $\Delta\mathbf{x}$ are not shown; they should be implicitly understood. Since each term in the sum over n equals its complex conjugate, P is explicitly real. For this reason, since the $n=0$ term does not contribute, we have changed the sum over n to a sum from $-\infty$ to ∞ at the expense of introducing an overall factor of $\frac{1}{2}$ into the formula. From here on this sum will simply be denoted by $\sum_n$.

It is possible to carry out both the sum over n and the integral over solid angle in closed form. To see this, consider the integral

$$I(t,\mathbf{r}) \equiv \sum_n \omega_n\int d\Omega\, e^{i\omega_n(t-\Omega\cdot\mathbf{r})} . \tag{3.10}$$

The integral over solid angle $\int d\Omega\, e^{i\Omega\cdot z}$ is easily evaluated, and equals $4\pi\sin(|\mathbf{z}|)/|\mathbf{z}|$. Hence one has

$$I(t,\mathbf{r})=\frac{4\pi}{|\mathbf{r}|}\sum_n e^{i\omega_n t}\sin\omega_n|\mathbf{r}| \ . \tag{3.11}$$

Because of the absolute value signs that appear, some care is required to obtain this last result—one must separately consider both possible signs of ω_n. The sum over n may now be explicitly carried out. Using the standard formula $\sum_n e^{in\theta}=2\pi\delta_p(\theta)$ for the periodic δ function on the interval $[-\pi,\pi)$, one obtains

$$I(t,\mathbf{r})=\frac{4\pi^2}{i|\mathbf{r}|}[\delta_p(4\pi(t+|\mathbf{r}|))-\delta_p(4\pi(t-|\mathbf{r}|))] \ . \tag{3.12}$$

Noting further that the periodic δ function may be expressed in terms of the ordinary Dirac δ function as

$$\delta_p(x)=\sum_{k=-\infty}^{\infty}\delta(x+2\pi k) \ , \tag{3.13}$$

and noting that $|\mathbf{r}|$ is always positive, one may combine the two δ functions in (3.12) to give

$$\begin{aligned} I(t,\mathbf{r})&=\frac{\pi}{i|\mathbf{r}|}\sum_{k=-\infty}^{\infty}[\delta(t+k/2+|\mathbf{r}|)-\delta(t+k/2-|\mathbf{r}|)] \\ &=2\pi i\sum_{k=-\infty}^{\infty}\epsilon(t+k/2)\delta((t+k/2)^2-|\mathbf{r}|^2) \ , \end{aligned} \tag{3.14}$$

where $\epsilon(x)=2\theta(x)-1$ is $+1$ for $x>0$ and -1 for $x<0$. From the definition (3.10) of $I(t,\mathbf{r})$ it is clear that applying the derivative operator $-i\partial/\partial t$ brings down an additional factor of ω_n. Inserting the time derivative of (3.14) into (3.8) leads to

$$P=4G\mu^2\sum_{k=-\infty}^{\infty}\int_0^1 du\int_0^1 dv\int_0^1 d\tilde{u}\int_0^1 d\tilde{v}\,\psi(u,v,\tilde{u},\tilde{v})\frac{\partial}{\partial\Delta t}\epsilon(\Delta t+k/2)\delta((\Delta t+k/2)^2-|\Delta\mathbf{x}|^2) \ . \tag{3.15}$$

In this expression the dependence of Δt and $\Delta\mathbf{x}$ on the four variables u, v, $\tilde{u}$, and $\tilde{v}$ has not been explicitly shown. The derivative operator $\partial/\partial\Delta t$ means *first* take the derivative of $I(t,\mathbf{r})$ with respect to the first argument, *then* substitute in the functions Δt and $\Delta\mathbf{x}$. Alternatively, it refers to any combination of derivative operators in (3.8) which will bring down a factor of $i\omega_n$.

It is possible to reexpress the sum over k of these four integrals as a single integral, simply by shifting one of the integration variables to the range $-\infty$ to ∞. For example, if we choose to shift $\tilde{v}$, then because the functions $\mathbf{a}$ and $\mathbf{b}$ are periodic, it is easy to see that $\Delta\mathbf{x}(u,v,\tilde{u},\tilde{v}-k)=\Delta\mathbf{x}(u,v,\tilde{u},\tilde{v})$ and that $\psi(u,v,\tilde{u},\tilde{v}-k)=\psi(u,v,\tilde{u},\tilde{v})$. However, the time function is *not* periodic; one has $\Delta t(u,v,\tilde{u},\tilde{v}-k)=\Delta t(u,v,\tilde{u},\tilde{v})+k/2$. Since the period of the loop is $\frac{1}{2}$, the energy radiated in a single oscillation of the loop is thus given by $E=P/2$:

$$E=2G\mu^2\int_0^1 du\int_0^1 dv\int_0^1 d\tilde{u}\int_{-\infty}^{\infty} d\tilde{v}\,\psi(u,v,\tilde{u},\tilde{v})\frac{\partial}{\partial\Delta t}\epsilon(\Delta t)\delta((\Delta t)^2-|\Delta\mathbf{x}|^2) \ . \tag{3.16}$$

Note that the choice to shift $\tilde{v}$ was arbitrary; we could have chosen to shift any one of the four integration variables. If we had chosen to shift some other variable, the only changes to (3.16) would be that the integration range for $\tilde{v}$ would be from 0 to 1, and the integration range of the new shifted variable would be from $-\infty$ to ∞. This expression for the energy radiated into gravitational radiation during one oscillation of the cosmic-string loop can be evaluated exactly in the case of piecewise linear string loops.

To make this formula directly useful, one must replace the operation $\partial/\partial\Delta t$ by an explicit operation in terms of derivatives with respect to the variables u, v, $\tilde{u}$, and $\tilde{v}$. The desired effect of this operation is to bring down a factor of $i\omega_n$ when applied to $\exp(i\omega_n[\Delta t(u,v,\tilde{u},\tilde{v})-\Omega\cdot\Delta x(u,v,\tilde{u},\tilde{v})])$. Let us denote this operation by

$$D(u,v,\tilde{u},\tilde{v})\equiv U(u,v,\tilde{u},\tilde{v})\partial_u+V(u,v,\tilde{u},\tilde{v})\partial_v-\tilde{U}(u,v,\tilde{u},\tilde{v})\partial_{\tilde{u}}-\tilde{V}(u,v,\tilde{u},\tilde{v})\partial_{\tilde{v}} \ , \tag{3.17}$$

where the functions U, V, $\tilde{U}$, and $\tilde{V}$ are determined by the desired effect of D on the exponential:

$$D\exp(i\omega_n[\Delta t-\Omega\cdot\Delta\mathbf{x}])=i\omega_n\exp(i\omega_n[\Delta t-\Omega\cdot\Delta\mathbf{x}]) \ . \tag{3.18}$$

Because D is chosen to be a linear differential operator, (3.18) is equivalent to the four equations

$$D\Delta t(u,v,\tilde{u},\tilde{v})=1 \quad\text{and}\quad D\Delta\mathbf{x}(u,v,\tilde{u},\tilde{v})=\mathbf{0} \ . \tag{3.19}$$

Substituting in the definitions of Δt and $\Delta\mathbf{x}$, this may be written as the 4×4 matrix equation

$$\begin{bmatrix} 1 & 1 & 1 & 1 \\ \mathbf{a}'(u) & \mathbf{b}'(v) & \mathbf{a}'(\tilde{u}) & \mathbf{b}'(\tilde{v}) \end{bmatrix}\begin{bmatrix} U \\ V \\ \tilde{U} \\ \tilde{V} \end{bmatrix}=\begin{bmatrix} 2 \\ \mathbf{0} \end{bmatrix} \ . \tag{3.20}$$

The solution to these linear equations yields the following expression for the differential operator D:

$$D(u,v,\tilde{u},\tilde{v}) = 2\frac{\mathbf{b}'(v)\cdot[\mathbf{a}'(\tilde{u})\times\mathbf{b}'(\tilde{v})]\partial_u - \mathbf{a}'(u)\cdot[\mathbf{a}'(\tilde{u})\times\mathbf{b}'(\tilde{v})]\partial_v - \mathbf{a}'(u)\cdot[\mathbf{b}'(v)\times\mathbf{b}'(\tilde{v})]\partial_{\tilde{u}} + \mathbf{a}'(u)\cdot[\mathbf{b}'(v)\times\mathbf{a}'(\tilde{u})]\partial_{\tilde{v}}}{\mathbf{b}'(v)\cdot[\mathbf{a}'(\tilde{u})\times\mathbf{b}'(\tilde{v})] - \mathbf{a}'(u)\cdot[\mathbf{a}'(\tilde{u})\times\mathbf{b}'(\tilde{v})] + \mathbf{a}'(u)\cdot[\mathbf{b}'(v)\times\mathbf{b}'(\tilde{v})] - \mathbf{a}'(u)\cdot[\mathbf{b}'(v)\times\mathbf{a}'(\tilde{u})]} . \tag{3.21}$$

In terms of the operator D, the energy radiated in gravitational waves during one oscillation of the string loop is given by

$$E = 2G\mu^2\int_0^1 du\int_0^1 dv\int_0^1 d\tilde{u}\int_{-\infty}^{\infty} d\tilde{v}\, \psi(u,v,\tilde{u},\tilde{v}) D(u,v,\tilde{u},\tilde{v})[\epsilon(\Delta t)\delta((\Delta t)^2 - |\Delta\mathbf{x}|^2)] . \tag{3.22}$$

In this expression the differential operator D acts on all the quantities that stand to its right.

Before continuing we note that half the terms may be easily eliminated from (3.22). Under the operation of interchanging the variables (u,v) with $(\tilde{u},\tilde{v})$, $U(\tilde{u},\tilde{v},u,v)=\tilde{U}(u,v,\tilde{u},\tilde{v})$, $V(\tilde{u},\tilde{v},u,v)=\tilde{V}(u,v,\tilde{u},\tilde{v})$, and $\Delta t(\tilde{u},\tilde{v},u,v) = -\Delta t(u,v,\tilde{u},\tilde{v})$, while $\psi(\tilde{u},\tilde{v},u,v)=\psi(u,v,\tilde{u},\tilde{v})$ and the arguments of the δ function are invariant. Using these results we interchange the variables (u,v) with $(\tilde{u},\tilde{v})$ in the first two terms of E in (3.22). Recalling that we could have shifted any one of the integration variables in (3.15), as explained following (3.16), one finds that

$$\int_0^1 du\int_0^1 dv\int_0^1 d\tilde{u}\int_{-\infty}^{\infty} d\tilde{v}\, \psi(u,v,\tilde{u},\tilde{v})(U\partial_u + V\partial_v)[\epsilon(\Delta t)\delta((\Delta t)^2 - |\Delta\mathbf{x}|^2)]$$
$$= \int_0^1 du\int_0^1 dv\int_0^1 d\tilde{u}\int_{-\infty}^{\infty} d\tilde{v}\, \psi(u,v,\tilde{u},\tilde{v})(\tilde{U}\partial_{\tilde{u}} + \tilde{V}\partial_{\tilde{v}})[\epsilon(-\Delta t)\delta((\Delta t)^2 - |\Delta\mathbf{x}|^2)] . \tag{3.23}$$

This equation, along with $\epsilon(-x) = -\epsilon(x)$, may now be used in (3.22) to eliminate two of the four terms in the operator D, yielding

$$E = 4G\mu^2\int_0^1 du\int_0^1 dv\int_0^1 d\tilde{u}\int_{-\infty}^{\infty} d\tilde{v}\, \psi(u,v,\tilde{u},\tilde{v})(U\partial_u + V\partial_v)[\epsilon(\Delta t)\delta((\Delta t)^2 - |\Delta\mathbf{x}|^2)] . \tag{3.24}$$

Although (3.24) has only half as many terms as (3.22), it is not the most useful form for our purposes.

The most convenient expression for E is obtained by replacing $\epsilon(\Delta t)$ in (3.22) by $2\theta(\Delta t)$. The $\epsilon(\Delta t) = 2\theta(\Delta t) - 1$ term can be replaced by $2\theta(\Delta t)$ because the -1 term makes no contribution to the integral. To see this, consider the effect of replacing $\epsilon(\Delta t)$ by -1 in (3.22). Denoting this by $E_{(-1)}$ and again using the transformation properties of $U(u,v,\tilde{u},\tilde{v})$, $V(u,v,\tilde{u},\tilde{v})$, $\psi(u,v,\tilde{u},\tilde{v})$, and the arguments of the δ function under the operation of interchanging the variables (u,v) with $(\tilde{u},\tilde{v})$, one finds that

$$E_{(-1)} \equiv -2G\mu^2\int_0^1 du\int_0^1 dv\int_0^1 d\tilde{u}\int_{-\infty}^{\infty} d\tilde{v}\, \psi(u,v,\tilde{u},\tilde{v})(U\partial_u + V\partial_v - \tilde{U}\partial_{\tilde{u}} - \tilde{V}\partial_{\tilde{v}})\delta((\Delta t)^2 - |\Delta\mathbf{x}|^2)$$
$$= -2G\mu^2\int_0^1 du\int_0^1 dv\int_0^1 d\tilde{u}\int_{-\infty}^{\infty} d\tilde{v}\, \psi(u,v,\tilde{u},\tilde{v})(\tilde{U}\partial_{\tilde{u}} + \tilde{V}\partial_{\tilde{v}} - \tilde{U}\partial_{\tilde{u}} - \tilde{V}\partial_{\tilde{v}})\delta((\Delta t)^2 - |\Delta\mathbf{x}|^2) = 0 . \tag{3.25}$$

This proves that $E_{(-1)} = 0$ and thus that $\epsilon(\Delta t)$ in (3.22) can be replaced by $2\theta(\Delta t)$.

The integration range $\tilde{v}\in(-\infty,\infty)$ in the expression for E (3.22) may be replaced by the finite range $\tilde{v}\in[-2,2]$. This is because the integrand of (3.22) vanishes unless $\tilde{v}\in[-2,2]$. Physically this is because in the center-of-mass frame, the string loop remains centered about a fixed coordinate location. Since the δ function has its support only on the light cone, it is impossible for regions of the string located far in the past or future to interact. To see this result mathematically, first consider the argument of the θ function. The only contributions to E arise when this argument is positive, i.e., when

$$u + v - \tilde{u} - \tilde{v} \ge 0 . \tag{3.26}$$

Since all three integration variables $u,v,\tilde{u}$ lie in the range [0,1], the θ function vanishes unless the variable $\tilde{v}$ lies in the range $\tilde{v}\in(-\infty,2]$. Further restrictions arise from considering the argument of the δ function. The only contributions to E arise when this argument vanishes, i.e., when

$$(u + v - \tilde{u} - \tilde{v})^2 = [\mathbf{a}(u) - \mathbf{a}(\tilde{u}) + \mathbf{b}(v) - \mathbf{b}(\tilde{v})]^2 . \tag{3.27}$$

However since the total length of the a loop is 1, the maximum length of the vector $\mathbf{a}(u) - \mathbf{a}(\tilde{u})$ is $\frac{1}{2}$. Similarly, the maximum length of the vector $\mathbf{b}(v) - \mathbf{b}(\tilde{v})$ is $\frac{1}{2}$. Hence the largest possible value of the right-hand side (RHS) of (3.27) is 1. This shows that the integrand vanishes unless the quantity

$$u + v - \tilde{u} - \tilde{v} \in [-1,1] . \tag{3.28}$$

Again making use of the possible ranges of u, v, and $\tilde{u}$ this implies that the δ function vanishes unless $\tilde{v}\in[-2,3]$. Combined with the restrictions arising from the θ function, this implies that the only contributions to E arise from the range $\tilde{v}\in[-2,2]$. Thus we obtain the final form of our result

$$E = 4G\mu^2\int_0^1 du\int_0^1 dv\int_0^1 d\tilde{u}\int_{-2}^{2} d\tilde{v}\, \psi(u,v,\tilde{u},\tilde{v}) D(u,v,\tilde{u},\tilde{v})[\theta(\Delta t)\delta((\Delta t)^2 - |\Delta\mathbf{x}|^2)] . \tag{3.29}$$

The expression just obtained has an interesting physical interpretation.

The string loses energy to gravitational waves precisely because of the gravitational self-interaction of the string with itself. From this point of view, the integral over $(\tilde{u},\tilde{v})$ in (3.29) is an integral over the sources [the stress tensor of the string world sheet at $x^{\alpha}(\tilde{u},\tilde{v})$] that create a metric perturbation at the space-time point $x^{\alpha}(u,v)$. The metric perturbation at $x^{\alpha}(u,v)$ is obtained by multiplying the source times a retarded propagator and integrating over the entire history of the source: the part of the world sheet that can contribute is covered by the coordinates $\tilde{u}\in[0,1]$ and $\tilde{v}\in[-2,2]$. The metric perturbations from the loop at one space-time point propagate along the light cone from that point to interact with some other point on the loop at some later time. The product $\theta\delta/2\pi$ that appears in (3.29) is precisely the retarded propagator (Eq. 12.133 of [16]). This creates the mechanism for energy loss: the string must do work against the tidal forces created by the metric perturbations due to the string itself. The energy lost in a single oscillation is obtained by integrating this work over the region on the string's world tube covered by the coordinates $u\in[0,1]$ and $v\in[0,1]$. Thus, the loss of energy due to gravitational radiation may be thought of in terms of a loop which creates metric perturbations, interacting with a loop whose motion does work against these perturbations.

We will see in the following sections that (3.29) can be evaluated *exactly* in *closed analytic form* for any piecewise linear cosmic string loop. The value of γ is then given immediately by (1.1).

IV. PIECEWISE LINEAR LOOPS

We now restrict our attention to piecewise linear loops. These are loops for which the functions $\mathbf{a}(u)$ and $\mathbf{b}(v)$, which define the loop's trajectory, are piecewise linear functions. The functions $\mathbf{a}(u)$ and $\mathbf{b}(v)$ may be pictured as a pair of closed loops, which consist of joined straight *segments.* The segments on the a and b loops join together at *kinks* where $\mathbf{a}'(u)$ and $\mathbf{b}'(v)$ are discontinuous. The a loop has N_a linear segments, and the b loop has N_b linear segments. Part of a typical a loop is shown in Fig. 1.

The following conventions, also shown in Fig. 1, are used to describe piecewise linear loops. The coordinate u on the a loop is chosen to take the value zero at one of the kinks, and increases along the loop. The *kinks* on the loop are labeled by the index i where $i=0,1,2,\ldots,N_a-1$. The value of u at the ith kink is denoted by u_i. Without loss of generality we set $u_0=0$. The *segments* on the loop are also labeled by the index i; the ith segment is the one lying between the ith kink and the $(i+1)$th kink. The kink at $u=u_{N_a}$ is the same as the first kink at $u=u_0=0$. Since $|\mathbf{a}'|^2=1$, the a loop has length 1. Thus, even though u_0 and u_{N_a} are at the same position on the loop, $u_0=0$ while $u_{N_a}=1$. The entire range $u\in(-\infty,\infty)$ may be covered by allowing the

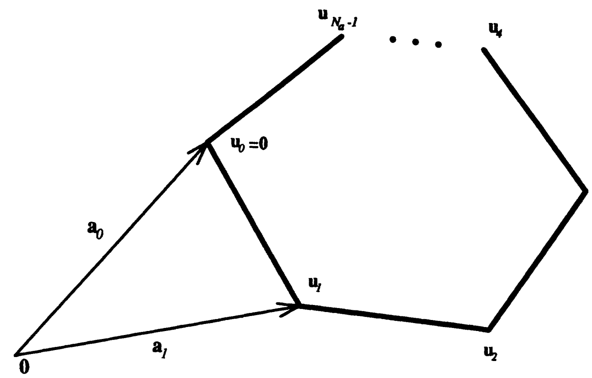

FIG. 1. For piecewise linear loops, the a and b loops consist of straight segments. The segments are joined together at kinks where $\mathbf{a}'(u)$ and $\mathbf{b}'(v)$ are discontinuous. The kinks on the a loop are labeled by the index i. The spatial position of kink i is $\mathbf{a}_i$. The value of the coordinate u at the ith kink is u_i. The segments on the a loop are also labeled by the index i; the ith segment being the one between the ith and the $(i+1)$th kink.

coordinate u to continue around the a loop in a periodic way. This also extends the range of the index to $i\in\mathbb{Z}$. Thus, for example, $u_{-N_a}=-1$, $u_0=0$, $u_{N_a}=1$, $u_{2N_a}=2$, and so on are all located at the same position on the a loop. Because $|\mathbf{a}'(u)|=1$, the length of the linear segment between the kinks at u_i and u_{i+1} (the ith segment) is

$$\Delta u_i = u_{i+1}-u_i \ . \tag{4.1}$$

The loop's position $\mathbf{a}(u)$ at $u=u_i$ is denoted

$$\mathbf{a}_i=\mathbf{a}(u_i) \ . \tag{4.2}$$

The constant unit vector tangent to the ith segment (pointing in the direction of increasing u parameter) is denoted

$$\mathbf{a}_i'=\frac{\mathbf{a}_{i+1}-\mathbf{a}_i}{\Delta u_i} \ . \tag{4.3}$$

With these definitions, the function $\mathbf{a}(u)$ for $u\in[u_i,u_{i+1}]$ may be written

$$\mathbf{a}(u)=\mathbf{a}_i+\mathbf{a}_i'(u-u_i) \quad \text{for } u\in[u_i,u_{i+1}] \ . \tag{4.4}$$

Note that for consistency, putting $u=u_{i+1}$ in (4.4), one must have

$$\mathbf{a}_{i+1}=\mathbf{a}_i+\mathbf{a}_i'(\Delta u_i) \ . \tag{4.5}$$

Similar notation is used for the function $\mathbf{b}(v)$. For $v\in[v_j,v_{j+1}]$, the function $\mathbf{b}(v)$ may be written

$$\mathbf{b}(v)=\mathbf{b}_j+\mathbf{b}_j'(v-v_j) \quad \text{for } v\in[v_j,v_{j+1}] \ . \tag{4.6}$$

Thus the a loop is entirely specified by the quantities $\mathbf{a}_i$; from them one can obtain both $\Delta u_i=|\mathbf{a}_{i+1}-\mathbf{a}_i|$ and $\mathbf{a}_i'$ given by (4.3). Identical notation is used for the b loop.

The function $\psi(u,v,\tilde{u},\tilde{v})$ takes a special form in the case of piecewise linear loops. In general one has

$$\psi(u,v,\tilde{u},\tilde{v})=G^{\mu\nu}(u,v)G_{\mu\nu}(\tilde{u},\tilde{v})-\tfrac{1}{2}G^{\lambda}{}_{\lambda}(u,v)G^{\gamma}{}_{\gamma}(\tilde{u},\tilde{v})$$
$$=2[\partial_u x^{\mu}\partial_v x^{\nu}\partial_{\tilde{u}}\tilde{x}_{\mu}\partial_{\tilde{v}}\tilde{x}_{\nu}+\partial_u x^{\mu}\partial_v x^{\nu}\partial_{\tilde{u}}\tilde{x}_{\nu}\partial_{\tilde{v}}\tilde{x}_{\mu}-\partial_u x^{\lambda}\partial_v x_{\lambda}\partial_{\tilde{u}}\tilde{x}^{\gamma}\partial_{\tilde{v}}\tilde{x}_{\gamma}] , \tag{4.7}$$

where, again $x^{\alpha}=x^{\alpha}(u,v)$ and $\tilde{x}^{\alpha}=x^{\alpha}(\tilde{u},\tilde{v})$. For the purpose of evaluating integral (3.29) it is necessary to break up the integrations over $(u,v,\tilde{u},\tilde{v})$ into rectangular four-cells. Each four-cell is denoted by a set of indices (i,j,k,l). The indices refer to segments on the a and b loops, each of which defines a specific range for one of the coordinates $(u,v,\tilde{u},\tilde{v})$. The index i will always refer to the u coordinate, j to the v coordinate, k to the $\tilde{u}$ coordinate, and l to the $\tilde{v}$ coordinate. Within each cell, we may write the four-vectors and tangent vectors

$$\begin{aligned}&x^{\alpha}(u,v)=\tfrac{1}{2}[u+v,\mathbf{a}_i+\mathbf{a}'_i(u-u_i)+\mathbf{b}_j+\mathbf{b}'_j(v-v_j)],\\&\partial_u x^{\alpha}=\tfrac{1}{2}[1,\mathbf{a}'_i],\quad \partial_v x^{\alpha}=\tfrac{1}{2}[1,\mathbf{b}'_j],\end{aligned}\qquad \text{for } u\in[u_i,u_{i+1}] \text{ and } v\in[v_j,v_{j+1}] \tag{4.8}$$

and similarly

$$\begin{aligned}&x^{\alpha}(\tilde{u},\tilde{v})=\tfrac{1}{2}[\tilde{u}+\tilde{v},\mathbf{a}_k+\mathbf{a}'_k(\tilde{u}-u_k)+\mathbf{b}_l+\mathbf{b}'_l(\tilde{v}-v_l)],\\&\partial_{\tilde{u}}\tilde{x}^{\alpha}=\tfrac{1}{2}[1,\mathbf{a}'_k],\quad \partial_{\tilde{v}}\tilde{x}^{\alpha}=\tfrac{1}{2}[1,\mathbf{b}'_l],\end{aligned}\qquad \text{for } \tilde{u}\in[u_k,u_{k+1}] \text{ and } \tilde{v}\in[v_l,v_{l+1}] . \tag{4.9}$$

Using (4.8) and (4.9) in (4.7) we find that $\psi(u,v,\tilde{u},\tilde{v})$ is a constant, ψ_{ijkl}, when $(u,v,\tilde{u},\tilde{v})$ are in the intervals defined by the segments (i,j,k,l). For any set of segments (i,j,k,l), the constant ψ_{ijkl} is given by

$$\psi_{ijkl}=\tfrac{1}{8}[(-1+\mathbf{a}'_i\cdot\mathbf{a}'_k)(-1+\mathbf{b}'_j\cdot\mathbf{b}'_l)+(-1+\mathbf{a}'_i\cdot\mathbf{b}'_l)(-1+\mathbf{b}'_j\cdot\mathbf{a}'_k)-(-1+\mathbf{a}'_i\cdot\mathbf{b}'_j)(-1+\mathbf{b}'_l\cdot\mathbf{a}'_k)] . \tag{4.10}$$

Note that $\psi_{ijkl}\in[-1,5/4]$. Also note that ψ_{ijkl} vanishes when $(i-k) \bmod N_a=0$ or $(j-l) \bmod N_b=0$.

It is helpful to keep track of whether the indices in a given equation refer to kinks or segments on the a and b loops. For instance, u_i refers to the value of the parameter u at the ith kink on the a loop. Similarly, $\mathbf{a}_i$ denotes a vector from the origin to the kink at $u=u_i$ on the a loop. By contrast, $\mathbf{a}'_i$ is a unit vector parallel to a specific segment on the a loop. The indices on ψ_{ijkl} also refer to specific segments on the a and b loops. The segments define specific ranges for the coordinates $(u,v,\tilde{u},\tilde{v})$. Of course these ranges will change as the indices take on different values.

The formula (3.29) for the energy radiated in gravitational waves during one oscillation of the string loop may now be rewritten for the case of a piecewise linear loop. The integrals over $(u,v,\tilde{u},\tilde{v})$ in (3.29) may be broken up into a sum of integrals over the individual segments making up the a and b loops. Because ψ_{ijkl} is a constant in each of these integrals, it may be pulled out of the integration, giving

$$E=4G\mu^2\sum_{i=0}^{N_a-1}\sum_{j=0}^{N_b-1}\sum_{k=0}^{N_a-1}\sum_{l=-2N_b}^{2N_b-1}\psi_{ijkl}\int_{u_i}^{u_{i+1}}du\int_{v_j}^{v_{j+1}}dv\int_{u_k}^{u_{k+1}}d\tilde{u}\int_{v_l}^{v_{l+1}}d\tilde{v}\,D_{ijkl}(u,v,\tilde{u},\tilde{v})[\theta(\Delta t)\delta((\Delta t)^2-|\Delta\mathbf{x}|^2)] . \tag{4.11}$$

Note that the summation of l is not from $-\infty$ to ∞ but is only over the finite range corresponding to $\tilde{v}\in[-2,2]$ as shown following Eq. (3.28). Here

$$D_{ijkl}(u,v,\tilde{u},\tilde{v})=U_{ijkl}\partial_u+V_{ijkl}\partial_v-\tilde{U}_{ijkl}\partial_{\tilde{u}}-\tilde{V}_{ijkl}\partial_{\tilde{v}} , \tag{4.12}$$

where the coefficients of the derivative operators are constant on any (i,j,k,l) segment, and are given by

$$\begin{aligned}&U_{ijkl}=Q_{ijkl}\mathbf{b}'_j\cdot[\mathbf{a}'_k\times\mathbf{b}'_l] ,\quad \tilde{U}_{ijkl}=Q_{ijkl}\mathbf{a}'_i\cdot[\mathbf{b}'_j\times\mathbf{b}'_l] ,\\&V_{ijkl}=-Q_{ijkl}\mathbf{a}'_i\cdot[\mathbf{a}'_k\times\mathbf{b}'_l] ,\quad \tilde{V}_{ijkl}=-Q_{ijkl}\mathbf{a}'_i\cdot[\mathbf{b}'_j\times\mathbf{a}'_k] ,\end{aligned} \tag{4.13}$$

with (twice) the inverse determinant given by

$$Q_{ijkl}=2(\mathbf{b}'_j\cdot[\mathbf{a}'_k\times\mathbf{b}'_l]-\mathbf{a}'_i\cdot[\mathbf{a}'_k\times\mathbf{b}'_l]+\mathbf{a}'_i\cdot[\mathbf{b}'_j\times\mathbf{b}'_l]-\mathbf{a}'_i\cdot[\mathbf{b}'_j\times\mathbf{a}'_k])^{-1} . \tag{4.14}$$

Note that U_{ijkl}, V_{ijkl}, $\tilde{U}_{ijkl}$, and $\tilde{V}_{ijkl}$ are all constant for a given set (i,j,k,l). Again, note that the indices (i,j,k,l) in equations like (4.12) refer to specific straight segments on the a and b loops. They do *not* refer to the components of some tensor.

V. EVALUATING THE INTEGRALS

The four partial derivative operators in $D_{ijkl}(u,v,\tilde{u},\tilde{v})$ in (4.11) may be trivially integrated over u, v, $\tilde{u}$, or $\tilde{v}$. Carrying out these integrations, E takes the form

$$E=8G\mu^2\sum_{i=0}^{N_a-1}\sum_{j=0}^{N_b-1}\sum_{k=0}^{N_a-1}\sum_{l=-2N_b}^{2N_b-1}\psi_{ijkl}[U_{ijkl}(S^{(u)}_{i+1,j,k,l}-S^{(u)}_{i,j,k,l})+V_{ijkl}(S^{(v)}_{i,j+1,k,l}-S^{(v)}_{i,j,k,l})$$
$$-\tilde{U}_{ijkl}(S^{(\tilde{u})}_{i,j,k+1,l}-S^{(\tilde{u})}_{i,j,k,l})-\tilde{V}_{ijkl}(S^{(\tilde{v})}_{i,j,k,l+1}-S^{(\tilde{v})}_{i,j,k,l})] \ , \tag{5.1}$$

where the superscript on each S denotes the variable which has been integrated out in that term. The quantities $S^{(u)}_{ijkl}$, $S^{(v)}_{ijkl}$, $S^{(\tilde{u})}_{ijkl}$, and $S^{(\tilde{v})}_{ijkl}$ appearing in (5.1) may all be expressed in terms of a three-dimensional integral containing a δ function:

$$S(\Delta x,\Delta y,\Delta z,\tau,s,C(M,N,a,b,c,d),\beta_1,\beta_2,\beta_3,\beta_4,\beta_5,\beta_6,\beta_7)$$
$$=\int_0^{\Delta x}dx\int_0^{\Delta y}dy\int_0^{\Delta z}dz\ \theta(\tau+s(x+y-z))\delta(\beta_1 xz+\beta_2 yz+\beta_3 xy+\beta_4 z+\beta_5 x+\beta_6 y+\beta_7) \ . \tag{5.2}$$

Notice that the limits of integration have been shifted so that the lower limit is always zero. The function C is defined by

$$C(M,N,a,b,c,d)=\begin{cases}1 \ \text{ if } \dfrac{a-c-1}{M}=\dfrac{d-b}{N}=\text{integer} \ , \\ 2 \ \text{ if } \dfrac{a-c-1}{M}=\dfrac{d-b-1}{N}=\text{integer} \ , \\ 3 \ \text{ if } \dfrac{a-c+1}{M}=\dfrac{d-b-1}{N}=\text{integer} \ , \\ 4 \ \text{ if } \dfrac{a-c+1}{M}=\dfrac{d-b}{N}=\text{integer} \ , \\ 0 \ \text{ otherwise} \ .\end{cases} \tag{5.3}$$

The function S does not depend upon C, since C does not appear on the RHS of (5.2). However C provides a convenient means to later simplify certain special cases that arise. The quantities $S^{(u)}_{ijkl}$, $S^{(v)}_{ijkl}$, $S^{(\tilde{u})}_{ijkl}$, and $S^{(\tilde{v})}_{ijkl}$ are given in terms of S by

$$\begin{aligned}S^{(u)}_{ijkl}&=S(\Delta v_l,\Delta u_k,\Delta v_j,M_{ijkl},-1,C(N_b,N_a,l,k,j,i),(1-\mathbf{b}'_j\cdot\mathbf{b}'_l),(1-\mathbf{a}'_k\cdot\mathbf{b}'_j),(\mathbf{a}'_k\cdot\mathbf{b}'_l-1) \ , \\ &\quad(\mathbf{b}'_j\cdot\mathbf{N}_{ijkl}-M_{ijkl}),(M_{ijkl}-\mathbf{b}'_l\cdot\mathbf{N}_{ijkl}),(M_{ijkl}-\mathbf{a}'_k\cdot\mathbf{N}_{ijkl}),\tfrac{1}{2}(\mathbf{N}^2_{ijkl}-M^2_{ijkl})) \ , \\ S^{(v)}_{ijkl}&=S(\Delta u_k,\Delta v_l,\Delta u_i,M_{ijkl},-1,C(N_a,N_b,k,l,i,j),(1-\mathbf{a}'_i\cdot\mathbf{a}'_k),(1-\mathbf{a}'_i\cdot\mathbf{b}'_l),(\mathbf{a}'_k\cdot\mathbf{b}'_l-1) \ , \\ &\quad(\mathbf{a}'_i\cdot\mathbf{N}_{ijkl}-M_{ijkl}),(M_{ijkl}-\mathbf{a}'_k\cdot\mathbf{N}_{ijkl}),(M_{ijkl}-\mathbf{b}'_l\cdot\mathbf{N}_{ijkl}),\tfrac{1}{2}(\mathbf{N}^2_{ijkl}-M^2_{ijkl})) \ , \\ S^{(\tilde{u})}_{ijkl}&=S(\Delta v_j,\Delta u_i,\Delta v_l,M_{ijkl},+1,C(N_b,N_a,j,i,l,k),(1-\mathbf{b}'_j\cdot\mathbf{b}'_l),(1-\mathbf{a}'_i\cdot\mathbf{b}'_l),(\mathbf{a}'_i\cdot\mathbf{b}'_j-1) \ , \\ &\quad(M_{ijkl}-\mathbf{b}'_l\cdot\mathbf{N}_{ijkl}),(\mathbf{b}'_j\cdot\mathbf{N}_{ijkl}-M_{ijkl}),(\mathbf{a}'_i\cdot\mathbf{N}_{ijkl}-M_{ijkl}),\tfrac{1}{2}(\mathbf{N}^2_{ijkl}-M^2_{ijkl})) \ , \\ S^{(\tilde{v})}_{ijkl}&=S(\Delta u_i,\Delta v_j,\Delta u_k,M_{ijkl},+1,C(N_a,N_b,i,j,k,l),(1-\mathbf{a}'_i\cdot\mathbf{a}'_k),(1-\mathbf{a}'_k\cdot\mathbf{b}'_j),(\mathbf{a}'_i\cdot\mathbf{b}'_j-1) \ , \\ &\quad(M_{ijkl}-\mathbf{a}'_k\cdot\mathbf{N}_{ijkl}),(\mathbf{a}'_i\cdot\mathbf{N}_{ijkl}-M_{ijkl}),(\mathbf{b}'_j\cdot\mathbf{N}_{ijkl}-M_{ijkl}),\tfrac{1}{2}(\mathbf{N}^2_{ijkl}-M^2_{ijkl})) \ ,\end{aligned} \tag{5.4}$$

where we have defined

$$M_{ijkl}=u_i+v_j-u_k-v_l \quad \text{and} \quad \mathbf{N}_{ijkl}=\mathbf{a}_i+\mathbf{b}_j-\mathbf{a}_k-\mathbf{b}_l \ . \tag{5.5}$$

Note that the three remaining integrations in S may be done in any order. The relationships

$$\begin{aligned}S(\Delta x,\Delta y,\Delta z,\tau,s,\beta_1,\beta_2,\beta_3,\beta_4,\beta_5,\beta_6,\beta_7)&=S(\Delta y,\Delta x,\Delta z,\tau,s,\beta_2,\beta_1,\beta_3,\beta_4,\beta_6,\beta_5,\beta_7) \\ &=S(\Delta x,-\Delta z,-\Delta y,\tau,s,-\beta_3,\beta_2,-\beta_1,-\beta_6,\beta_5,-\beta_4,\beta_7)\end{aligned} \tag{5.6}$$

allow one to rewrite the integrations in any order.

It should be noted that in the definition (5.2) of S, there are no terms in the argument of the δ function that are quadratic in x, y, or z. This is because the terms u^2, v^2, $\tilde{u}^2$, and $\tilde{v}^2$ in $\Delta t^2-|\Delta\mathbf{x}|^2$ appear with respective coefficients

$$\begin{aligned}&-\tfrac{1}{2}(1-\mathbf{a}'_i\cdot\mathbf{a}'_i), \quad -\tfrac{1}{2}(1-\mathbf{b}'_j\cdot\mathbf{b}'_j) \ , \\ &-\tfrac{1}{2}(1-\mathbf{a}'_k\cdot\mathbf{a}'_k), \quad -\tfrac{1}{2}(1-\mathbf{b}'_l\cdot\mathbf{b}'_l) \ .\end{aligned} \tag{5.7}$$

It is easy to see that these coefficients all vanish since $|\mathbf{a}'|^2=|\mathbf{b}'|^2=1$. This is because, as described in Sec. II, the coordinates u and v are null coordinates.

VI. EVALUATION OF S

The previous section reduced the problem of determining γ in the piecewise linear case to evaluating a set of integrals defined by the function S in Eq. (5.2). In this section we carry out that evaluation in closed form. The δ function appearing in (5.2) allows us to reduce the number of integrations in S from three to two. This δ function may be written as $\delta(f(x,y,z))$, where the argument of the δ function is

$$f(x,y,z)=\beta_1 xz+\beta_2 yz+\beta_3 xy+\beta_4 z+\beta_5 x+\beta_6 y+\beta_7 \ . \tag{6.1}$$

The δ function will only have support when $f(x,y,z)=0$. Solving $f(x,y,z)=0$ for $x(y,z)$, $y(x,z)$, and $z(x,y)$, respectively, we find that

$$x(y,z)=-\frac{\beta_2 yz+\beta_4 z+\beta_6 y+\beta_7}{\beta_1 z+\beta_3 y+\beta_5} \ , \tag{6.2}$$

$$y(x,z)=-\frac{\beta_1 xz+\beta_5 x+\beta_4 z+\beta_7}{\beta_3 x+\beta_2 z+\beta_6} \ , \tag{6.3}$$

and

$$z(x,y)=-\frac{\beta_3 xy+\beta_5 x+\beta_6 y+\beta_7}{\beta_1 x+\beta_2 y+\beta_4} \ . \tag{6.4}$$

The surface $z(x,y)$ consists of a pair of disconnected hyperbolic sheets as shown in Fig. 2. The sheets are separated by the plane $\beta_1 x+\beta_2 y+\beta_4=0$, where the denominator of (6.4) vanishes. If these sheets pass through the region of integration of (5.2), which is a rectangular box with opposite corners (0,0,0) and $(\Delta x,\Delta y,\Delta z)$, then the δ function will have support in that region and S may contribute to E.

The hyperbolic sheets have a simple physical interpretation. For purposes of clarity we discuss the case $S^{\bar{i}\bar{j}}_{ijkl}$; the other three integrals in (5.4) have similar interpretations. The z coordinate in S parametrizes the world line followed by the kth kink on the string loop. This kink moves along a straight, null world line. The x,y integrations are over a (diamond-shaped) planar patch of the world tube, swept out by a linear segment of the string loop. Note that these patches are always timelike. The edges of this planar patch are bounded by the straight, null world lines of ith and jth kinks. The future and past light cones of any point on the kth kink's world line (i.e., fixed z) may intersect the planar patch bounded by the ith and jth kinks. Even if they fail to intersect this patch, they will intersect the infinite two-plane passing through the patch, which is parametrized by x and y. The intersection will trace out a hyperbola on the plane which may or may not intersect the actual x,y integration region. The hyperbola is given (with z fixed) by (6.3). This hyperbola corresponds to the intersection of a $z=$const plane with the hyperbolic sheets of Fig. 2. Because one branch of this hyperbola lies on the future light cone and the other lies on the past light cone, we refer to these as the *future branch* and the *past branch*. The two branches are disconnected except in the case where the plane passes through the origin of the light cone. In this case they touch at a single point—the apex of the light cone. As the apex moves along the world line of the kink (i.e., z increases) the light cone sweeps out a region on the x-y plane. This can be seen by taking successive $z=$const cross sections of the hyperbolic sheets, where the constant ranges from 0 to Δz. The region swept out in the x-y plane will be bounded by the hyperbolas $y(x,0)$ and $y(x,\Delta z)$. Note that if we restrict attention to just the future branches or just the past branches, then the $y(x,\Delta z)$ hyperbola always lies above (and to the right of) the $y(x,0)$ hyperbola in the x-y plane. Therefore, we refer to these as the "top" and "bottom" hyperbolas, as shown in Fig. 3. The hyperbolae shown in Fig. 3 will intersect the x,y integration region only if the hyperbolic sheets pass inside the integration box shown in Fig. 2.

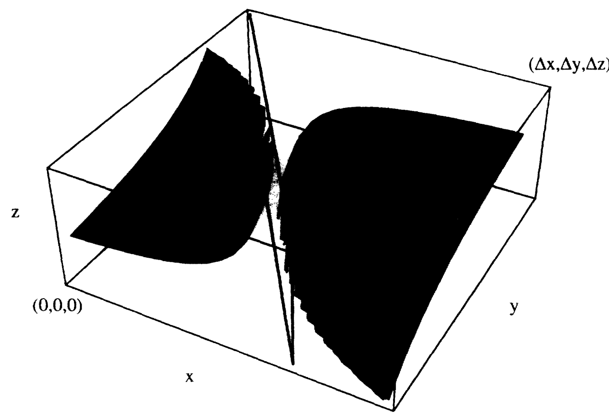

FIG. 2. The delta function $\delta[f(x,y,z)]$ which appears in (5.2) only has support when $f(x,y,z)=0$. Solving $f(x,y,z)=0$ for $z(x,y)$ we find that the surface $z(x,y)$ consists of a pair of disconnected hyperbolic sheets. The hyperbolic sheets are separated by the plane $\beta_1 x+\beta_2 y+\beta_4=0$, where the denominator of (6.4) vanishes. The intersection of a $z=$const plane with these sheets will be a hyperbola in the x-y plane. The integration volume for (5.2) is a box with opposite corners (0,0,0) and $(\Delta x,\Delta y,\Delta z)$.

There are two useful sets of conditions which can be checked immediately to see if S vanishes. These test whether the hyperbolic sheets $z(x,y)$ pass through the integration box. If the sheets do not pass through the box, then the δ function in (5.2) has no support, and S vanishes. One of the conditions applies for $s=+1$. In this case, the θ function in (5.2) restricts the integration to be over only the hyperbolic sheet swept out by the future light cone. The other condition applies for $s=-1$. In this case, the θ function in (5.2) restricts the integration to be over only the hyperbolic sheet swept out by the past light cone. If $s=+1$, then

$$S=0 \Longleftrightarrow (\tau+\Delta x+\Delta y\le 0) \ \text{or} \ (\beta_3\Delta x\Delta y+\beta_5\Delta x+\beta_6\Delta y+\beta_7\ge 0) \ \text{or} \ (\Delta z\le\tau \ \text{and} \ \beta_4\Delta z+\beta_7\le 0) \ . \tag{6.5}$$

Similarly, if $s=-1$, then

$$S=0 \Longrightarrow (\tau+\Delta x \le 0) \ \text{or} \ (\beta_4 \Delta z+\beta_7 \ge 0) \ \text{or} \ (\Delta x+\Delta y \le \tau \ \text{and} \ \beta_3 \Delta x \Delta y+\beta_5 \Delta x+\beta_6 \Delta y+\beta_7 \le 0) \ . \tag{6.6}$$

In practice, these conditions are frequently satisfied, so their implementation saves large amounts of computation.

It is straightforward to do the integral over z in (5.2) to eliminate the δ function in S. We make use of the standard formula

$$\int \delta(f(z)) g(z) dz=\sum_p g(z_p) \Big/ \left| \frac{\partial f}{\partial z}(z_p) \right| , \tag{6.7}$$

where the sum is taken over all the roots z_p of $f(z)$ that lie within the range of z integration. Because

$$\frac{\partial f}{\partial z}=\beta_1 x+\beta_2 y+\beta_4 , \tag{6.8}$$

the integration of (5.2) over z yields

$$S(\Delta x,\Delta y,\Delta z,\tau,s,C,\beta_1,\ldots,\beta_7)=\int_0^{\Delta x} dx \int_0^{\Delta y} dy \frac{\theta(z(x,y))\theta(\Delta z-z(x,y))\theta(\tau+s[x+y-z(x,y)])}{|\beta_1 x+\beta_2 y+\beta_4|} . \tag{6.9}$$

The first two θ functions in this equation arise from (6.7): the only roots included in the sum over p are those lying within the range $z \in [0,\Delta z]$ of z integration.

The integral (6.9) has a simple physical interpretation which is directly connected to the physical interpretation of (5.2) already given following Eq. (6.4). The x and y integrations are over a planar patch on the string loop's world tube, as in (5.2). The first two θ functions in (6.9) only have support between the hyperbolic curves $y(x,0)$ and $y(x,\Delta z)$ (i.e., the bottom and top curves) shown in Fig. 3. The curve $y(x,0)$ describes the intersection of the hyperbolic sheet shown in Fig. 2 with the bottom of the integration box. The curve $y(x,\Delta z)$ describes the intersection of the hyperbolic sheet with the top of the integration box. Thus, the first two θ functions in (6.9) will only have support if the hyperbolic sheets pass through the box of integration in (5.2). The third θ function in (6.9) effectively restricts the integration to be over the future branches $(s=+1)$ or the past branches $(s=-1)$ of the hyperbolas.

When evaluating (6.9), there are five different fundamental types of integrals that can arise depending upon the relative positions of the two hyperbolic curves $y(x,0)$ and $y(x,\Delta z)$ and the rectangular region in the x-y plane bounded by the opposite corners (0,0) and $(\Delta x,\Delta y)$. Each of the five possibilities are shown (using the future branches of the hyperbolas) in Fig. 4. Each type of integral may also occur with the past branches of the hyperbolas. The first type occurs when both hyperbolas (top and bottom) pass through the planar patch. The second type occurs when the entire planar patch lies between the two hyperbolas. A third possible type occurs when neither hyperbola passes through the planar patch and the planar patch does not lie between the two hyperbolas. For this type of integral, (6.9) has no support and vanishes. The last two types arise when one of the hyperbolas (top or bottom) passes through the planar patch but the other does not.

Remarkably, each of the fundamental integral types can be done analytically in closed form. To assist in this process, the x integration in (6.9) must be divided into consecutive ranges; the type of integral in each range is different. A systematic method for determining these integration ranges in x will be given next.

The dividing points (in x) between the successive ranges are determined by the four points at which the bottom and top hyperbolas $y(x,0)$ and $y(x,\Delta z)$ intersect the lines $y=0$ and $y=\Delta y$. We denote the x coordinates of the four intersection points by $\phi_1,\ldots,\phi_4$. The type of integral being done in (6.9) will change at each of the in-

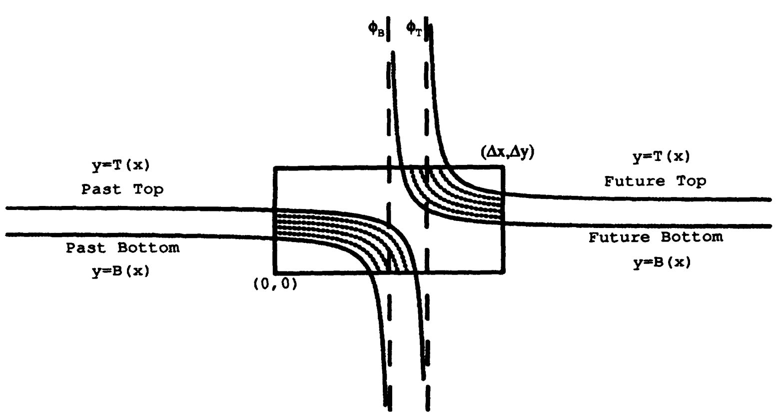

FIG. 3. The integrals (6.9) in the expression for the radiated power are over the rectangular region bounded by the corners (0,0) and $(\Delta x,\Delta y)$. Each integral contains three step functions. In the region of integration, the first two step functions are both nonzero only in the shaded regions between the "top" and "bottom" hyperbolas. The third step function is on in the region which includes the "future" branches if $s=1$ or the "past" branches if $s=-1$. The vertical asymptote of the bottom (top) hyperbola is shown as a dashed line that lies at $x=\phi_B$ $(x=\phi_T)$.

tersection points which is within the boundaries of the x integration, i.e., $0<x<\Delta x$. The boundaries of the x integration will be labeled ϕ_0 and ϕ_5. The x coordinates $\phi_1,\ldots,\phi_4$ are given by

$$\phi_1=x(0,\Delta z)=-\frac{\beta_4\Delta z+\beta_7}{\beta_1\Delta z+\beta_5} \quad \text{if } C\neq 1 \text{ or else } \phi_1=0\ ,$$
$$\phi_2=x(\Delta y,\Delta z)=-\frac{\Delta z(\beta_2\Delta y+\beta_4)+\beta_6\Delta y+\beta_7}{\beta_3\Delta y+\beta_1\Delta z+\beta_5} \quad \text{if } C\neq 2 \text{ or else } \phi_2=0\ , \tag{6.10}$$
$$\phi_3=x(\Delta y,0)=-\frac{\beta_6\Delta y+\beta_7}{\beta_3\Delta y+\beta_5} \quad \text{if } C\neq 3 \text{ or else } \phi_3=0\ ,$$
$$\phi_4=x(0,0)=-\frac{\beta_7}{\beta_5} \quad \text{if } C\neq 4 \text{ or else } \phi_4=0\ .$$

The values of C are checked because there are four special cases. In these special cases the formula given for one of $\phi_1,\ldots,\phi_4$ is indeterminate because the numerator and denominator in (6.10) vanish.

The conditions for the four special cases are given in the definition (5.3) of C. Physically, these special cases arise when end of the kink's world line, parametrized by z, touches one of the four corners of the diamond-shaped patch of the world sheet defined by the x and y integrations. The intersections of the future and past light cones of a point on the kink's world line with the plane defined by the diamond-shaped patch are usually hyperbolas. However, when the point on the kink's world line is also a corner of the diamond-shaped region, then the plane passes through the apex of the light cone and the hyperbola degenerates into a pair of straight lines. These straight lines will lie along the two edges of the planar patch which are joined at the corner where the kink's world line touches. For each of the four special cases, one of the formula for ϕ in (6.10) would become indeterminate. Consider, for instance, the case where the end of the kink's world line (i.e., $z=\Delta z$) touches the lower left corner of the integration region (i.e., $x=y=0$). At this point we have $x^\alpha(u,v)=x^\alpha(\tilde{u},\tilde{v})$. In this case the future top curve lies along the left and lower sides of the rectangular integration region. One can verify that in this case, both the numerator and denominator in the equation for ϕ_1 vanish. It is ϕ_1 that becomes indeterminate in this case because ϕ_1 is the x coordinate of the intersection of the top curve and the line $y=0$, which does not have a unique solution in this case. The other three special cases are similar. In each case a different ϕ would become indeterminate if the value of C were not checked.

All four special cases are dealt with in the same manner. The purpose of the ϕ's is to locate the x coordinates where the type of integral being done changes. However, since intersection curves which lie along the edges of the integration region never cause the type of integration being done to change, it is sufficient to simply set the corresponding ϕ_i to zero [or to any value outside the range (ϕ_0,ϕ_5)].

The support of the x integration in (6.9) may be less than the range $0<x<\Delta x$ because of the third θ function. Thus one does not always have $\phi_0=0$ and $\phi_5=\Delta x$. Because the integrations in (6.9) have support only between the future branches $(s=+1)$ or the past branches $(s=-1)$ of the hyperbolas, it is convenient to define ϕ_0 and ϕ_5 in a more general way. First, we define ϕ_B to be the vertical asymptote to the bottom hyperbola when $s=+1$ and zero otherwise, and ϕ_T to be the vertical asymptote to the top hyperbola when $s=-1$ and zero otherwise:

$$\begin{aligned}\phi_B&=\theta(s)x(y\to\infty,0)=-\theta(s)\frac{\beta_6}{\beta_3}\ ,\\ \phi_T&=\theta(-s)x(y\to\infty,\Delta z)\\ &=-\theta(-s)\frac{\beta_2\Delta z+\beta_6}{\beta_3}\ .\end{aligned}\tag{6.11}$$

The boundaries of the x integration are then defined to be

$$\begin{aligned}\phi_0&=\max(0,\phi_B)\ ,\\ \phi_5&=\min[\Delta x,\phi_T+\theta(s)\Delta x]\ .\end{aligned}\tag{6.12}$$

This definition of ϕ_0 and ϕ_5 eliminates regions of integration which only contain the past branches of the hyperbolas when $s=+1$ and regions which only contain the future branches of the hyperbolas when $s=-1$.

One may now express S as a sum of integrals over the successive ranges of the x integration. The set of points $\{\phi_0\cdots\phi_5\}$ partition the x integration into at most five ranges. Let $\{x_0,x_1,x_2,x_3,x_4,x_5\}$ be the increasing sort-

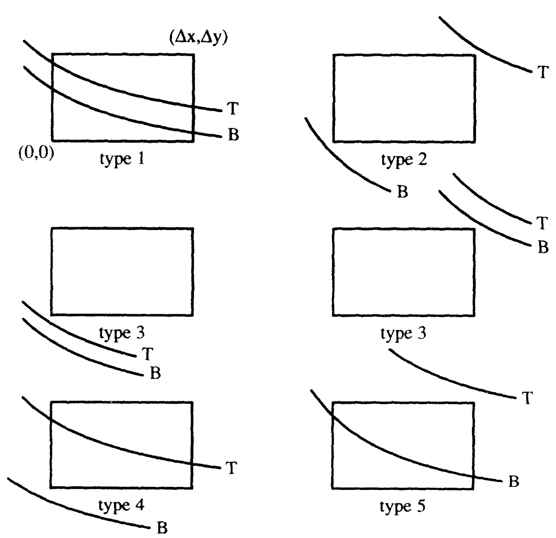

FIG. 4. The five different fundamental types of integrals that arise when evaluating (6.9). The type depends upon the relative positions of the two hyperbolic curves $y(x,0)$ (labeled B for "bottom") and $y(x,\Delta z)$ (labeled T for "top") and the rectangular region bounded by the opposite corners (0,0) and $(\Delta x,\Delta y)$. The five possibilities are shown using the future branches of the hyperbolas (the case for $s=+1$). Each type of integral may also occur with the past branches of the hyperbolas (for $s=-1$).

ed set of ϕ's,

$$\{x_0,x_1,x_2,x_3,x_4,x_5\} = \text{sort}(\{\phi_0,\phi_1,\phi_2,\phi_3,\phi_4,\phi_5\}) , \quad (6.13)$$

sorted so that $x_i \le x_{i+1}$. If we define the mid-point between two successive x's as

$$\bar{x}_n = (x_n + x_{n+1})/2 , \quad (6.14)$$

then we may rewrite the S integral (6.9) as a sum of integrals over each successive x range:

$$S(\Delta x,\Delta y,\Delta z,\tau,s,C,\beta_1,\ldots,\beta_7) = \sum_{n=0}^{4} \theta(\bar{x}_n - \phi_0)\theta(\phi_5 - \bar{x}_n) T(x_n,x_{n+1},\Delta y,\Delta z,\tau,s,\beta_1,\ldots,\beta_7) . \quad (6.15)$$

The two θ functions ensure that only the ranges of x between ϕ_0 and ϕ_5 may contribute. The function T is defined to be

$$T(x_l,x_u,\Delta y,\Delta z,\tau,s,\beta_1,\ldots,\beta_7) = \int_{x_l}^{x_u} dx \int_0^{\Delta y} dy \frac{\theta(z(x,y))\theta(\Delta z - z(x,y))\theta(\tau + s[x + y - z(x,y)])}{|\beta_1 x + \beta_2 y + \beta_4|} . \quad (6.16)$$

The reason that we have defined the function T is that the x integration being done in (6.16) is over a region which contains only one of the five possible fundamental types of integrals discussed in the paragraphs preceding equation (6.10) and shown in Fig. 4.

What remains is to find the analytic form of (6.16) for each of the five possible types of integrals that can arise. Recall that the different types of integrals arise, as shown in Fig. 4, from the different possible relative positions of the top and bottom hyperbolas compared to the (x,y) region of integration. If the region of integration is between the two hyperbolas, then the first two θ functions in (6.16) will have support over the entire region, and the limits of the y integration will run from 0 to Δy. If both hyperbolas pass through the region of integration, then the first two θ functions in (6.16) restrict the y limits of integration to run from $y(x,0)$ to $y(x,\Delta z)$. The last two types of integrals which give nonzero contributions are when one of the hyperbolas passes through the region of integration but the other does not. These types of integrals will have y limits of integration which run from 0 to $y(x,\Delta z)$ or from $y(x,0)$ to Δy depending on whether it is the top or the bottom hyperbola that passes through the region of integration. For each type of integral, the third θ function in (6.16) restricts the integration region to be between either the future ($s=+1$) or the past ($s=-1$) branches of the hyperbolae. If we make the definitions

$$\begin{aligned}
\bar{x} &= (x_l + x_u)/2 , \\
y_b &= s\, y(\bar{x},\theta(-s)\Delta z) , \\
y_t &= s\, y(\bar{x},\theta(s)\Delta z) , \\
y_l &= -\theta(-s)\Delta y , \\
y_u &= \theta(s)\Delta y , \\
\delta &= \epsilon(\beta_1 \bar{x} + s\beta_2 y_b + \beta_4) ,
\end{aligned} \quad (6.17)$$

then the integrals in (6.16) can be carried out for each of the five different cases. One obtains

$$T(x_l,x_u,\Delta y,\Delta z,\tau,s,\beta_1,\ldots,\beta_7)$$

$$= \begin{cases}
\displaystyle\int_{x_l}^{x_u} dx \int_0^{\Delta y} dy \frac{1}{|\beta_1 x + \beta_2 y + \beta_4|} = \frac{\delta}{\beta_2}[L(x_l,x_u,\beta_1,\beta_4 + \beta_2 \Delta y) - L(x_l,x_u,\beta_1,\beta_4)] \\
\qquad \text{for } y_t \le y_b \le y_l \text{ or for } y_b \le y_l \text{ and } y_u \le y_t \\
\displaystyle\int_{x_l}^{x_u} dx \int_{\theta(-s)y(x,0)}^{\theta(s)y(x,\Delta z)+\theta(-s)\Delta y} dy \frac{1}{|\beta_1 x + \beta_2 y + \beta_4|} = \frac{s\delta}{\beta_2}[Q(x_l,x_u,\beta_1\beta_3,\beta_1\beta_6 + \beta_3\beta_4 - \beta_2\beta_5,\beta_4\beta_6 - \beta_2\beta_7) \\
\qquad - L(x_l,x_u,\beta_3,\beta_6 + \beta_2\theta(s)\Delta z) - L(x_l,x_u,\beta_1,\beta_4 + \beta_2\theta(-s)\Delta y)] \\
\qquad \text{for } y_b \le y_l < y_t < y_u \\
\displaystyle\int_{x_l}^{x_u} dx \int_{y(x,0)}^{y(x,\Delta z)} dy \frac{1}{|\beta_1 x + \beta_2 y + \beta_4|} = \frac{\delta}{\beta_2}[L(x_l,x_u,\beta_3,\beta_6) - L(x_l,x_u,\beta_3,\beta_6 + \beta_2 \Delta z)] \qquad \text{for } y_l < y_b < y_t < y_u \\
\displaystyle\int_{x_l}^{x_u} dx \int_{\theta(s)y(x,0)}^{\theta(-s)y(x,\Delta z)+\theta(s)\Delta y} dy \frac{1}{|\beta_1 x + \beta_2 y + \beta_4|} = \frac{s\delta}{\beta_2}[L(x_l,x_u,\beta_3,\beta_6 + \beta_2\theta(-s)\Delta z) + L(x_l,x_u,\beta_1,\beta_4 + \beta_2\theta(s)\Delta y) \\
\qquad - Q(x_l,x_u,\beta_1\beta_3,\beta_1\beta_6 + \beta_3\beta_4 - \beta_2\beta_5,\beta_4\beta_6 - \beta_2\beta_7)] \\
\qquad \text{for } y_l < y_b < y_u \le y_t \text{ or for } y_l < y_b < y_u \text{ and } y_t \le y_b \\
0 \quad \text{for } y_u \le y_b \text{ or for } y_b < y_t \le y_l .
\end{cases}$$

(6.18)

Here, the functions L and Q are the "linear" and "quadratic" integrals defined by

$$L(x_1,x_2,c_1,c_0)=\int_{x_1}^{x_2} dx\,\ln|c_1x+c_0|=\begin{cases}\left[\left[x+\frac{c_0}{c_1}\right]\ln|c_1x+c_0|-x\right]_{x_1}^{x_2} & \text{for } c_1\neq 0\\ (x_2-x_1)\ln|c_0| & \text{for } c_1=0\end{cases} \tag{6.19}$$

and

$$Q(x_1,x_2,c_2,c_1,c_0)=\int_{x_1}^{x_2} dx\,\ln|c_2x^2+c_1x+c_0|$$

$$=\begin{cases} L(x_1,x_2,c_1,c_0) \quad \text{for } c_2=0\\ L\left[x_1,x_2,1,\frac{c_1+\sqrt{c_1^2-4c_0c_2}}{2c_2}\right]+L\left[x_1,x_2,1,\frac{c_1-\sqrt{c_1^2-4c_0c_2}}{2c_2}\right]+(x_2-x_1)\ln|c_2| \\ \qquad\qquad\qquad\qquad\qquad\qquad\qquad\qquad\qquad\qquad \text{for } 0\le c_1^2-4c_0c_2\\ \left\{x\ln\left[x^2+\frac{4c_0c_2-c_1^2}{4c_2^2}\right]-2x+2\left[\frac{4c_0c_2-c_1^2}{4c_2^2}\right]^{1/2}\arctan\left[x\left[\frac{4c_2^2}{4c_0c_2-c_1^2}\right]^{1/2}\right]\right\}_{x_1+c_1/2c_2}^{x_2+c_1/2c_2}\\ +L\left[x_1+\frac{c_1}{2c_2},x_2+\frac{c_1}{2c_L},0,c_2\right] \qquad\qquad\qquad\qquad\qquad \text{for } c_1^2-4c_0c_2<0\ . \end{cases} \tag{6.20}$$

Thus T, and hence S has been evaluated analytically for all possible cases. Using the results of this section, one can carry out the summations in (5.1) to arrive at a final value for γ; the power radiated in gravitational waves by a string loop.

VII. TESTING THE FORMULA FOR γ AGAINST PREVIOUS RESULTS

In this section we compare the γ values given by our formulas to previously published values for a large number of loop trajectories. The formulas obtained in Secs. V and VI were directly implemented by computer code. In some cases we find disagreement between our results and those previously published. There are, in fact, several cases where conflicting results have been published for the same loop trajectories. In the cases where a disagreement was found, we have identified the errors made in the published work which led to the incorrect results. In these cases our formulas give the correct values of γ. We are confident that they are correct because, in every case, we have shown our results to be consistent with those given by other independent methods. The other methods used to confirm our results were the FFT method of Allen and Shellard [14] and/or a corrected implementation of the numerical method used by the original author(s).

While our formulas handle piecewise linear loops exactly, most of the previous work in this area has considered smooth cosmic string trajectories (typically providing analytic expressions for the a and b loops). To compare the results of our formulas to the published values of γ for these smooth loops, we calculate γ for piecewise linear loop trajectories of approximately the same shape. If the number of segments used (N_a and N_b) is reasonably large, then the piecewise linear loop trajectory and the smooth loop trajectory will be very similar in shape, and we expect that the values of γ for the two trajectories will be very close. An example of how we generate specific piecewise linear trajectories is given later in this section. The rate at which γ converges as the number of linear segments is increased is also discussed.

Prior to this work the only fully analytic closed form solution for γ for any string loop trajectory was given by Garfinkle and Vachaspati [11]. They considered the piecewise linear loops defined by a and b loops which consisted of just two linear segments each; i.e., $N_a=N_b=2$. This defines a family of loop trajectories which depend on a single parameter ϕ, the angle between the a and b loops. As a function of ϕ,γ is given by

$$\gamma(\phi)=\frac{32}{\sin^2\phi}\left[(1+\cos\phi)\ln\left[\frac{2}{1+\cos\phi}\right]+(1-\cos\phi)\ln\left[\frac{2}{1-\cos\phi}\right]\right]. \tag{7.1}$$

When calculating γ with our formulas, we used a and b loops with three segments (where the length of the third segment was much smaller than the other two). This was necessary in order to prevent a singularity; exactly parallel segments cause the determinant in (4.14) to vanish. Equation (7.1) is plotted in Fig. 5 (solid line) along with the γ values (dots) given by our code for a number of loops with different values of ϕ. Since these are piecewise linear loops we expect our results to be highly accurate. Indeed, the points plotted in Fig. 5 showing our results had to be enlarged in order to distinguish them from the plot of (7.1). Thus our method completely confirms the results of Garfinkle and Vachaspati.

The next set of loop trajectories which we use to test our formulas is a three-parameter family of trajectories first examined by Burden [10]. The three parameters are

L, M, and ϕ, where L and M are positive integers and ϕ is an angle in the range $[0,\pi]$. The Burden trajectories are defined by the a and b loops:

$$\mathbf{a}(u)=\frac{L^{-1}}{2\pi}[\cos(2\pi Lu)\hat{\mathbf{z}}+\sin(2\pi Lu)(\cos\phi\hat{\mathbf{x}}+\sin\phi\hat{\mathbf{y}})] ,$$
$$\mathbf{b}(v)=\frac{M^{-1}}{2\pi}[\cos(2\pi Mv)\hat{\mathbf{z}}-\sin(2\pi Mv)\hat{\mathbf{x}}] . \tag{7.2}$$

The b loop winds M times around a circle in the x-z plane. The a loop winds L times around a circle whose plane is at an angle ϕ with respect to the x-z plane. The Burden string loops are nonintersecting cuspy loops in the case $M=1,L>1$ and ϕ not equal to 0 or π. Burden calculated values of γ for loops with $M=1$ and $L=1,2,3,5,15$ for several values of ϕ. The values of γ for loops with $M=1$ and $L=3,5$ were also calculated by Quashnock and Spergel [13]. Using our formula we calculated the values of γ for a large number of loops, each of which is a piecewise linear approximation to a Burden loop. In addition, we calculated a number of γ values using the FFT method of Allen and Shellard [14]. Our results for loops with $M=1$ and $L=3,5$ are shown in Fig. 6 along with the results of Burden, Quashnock, and Spergel, and the FFT method. We find excellent agreement among all four sets of results. This also shows that piecewise linear loops with fairly small numbers of segments ($N_a=16L$ and $N_b=16M=16$) can provide excellent approximations to smooth loop trajectories and provides further evidence that our formulas are correct.

Values of γ for the Burden loops with $L=M=1$ have been published by Burden [10], Vachaspati and Vilenkin [9], and Durrer [8]. These results, along with the results of the FFT method and our new method are shown in Fig. 7. There is excellent agreement between four of the sets of results. However, Durrer's results for these trajectories do not agree well with the others.

To understand why Durrer's results do not agree with the others we recalculated γ for these trajectories using the same numerical method used by Burden, Vachaspati and Vilenkin, and Durrer. This method requires one to calculate the average power radiated by a string loop using the formula previously given in (3.7):

$$P=\sum_{n=1}^{\infty}\int d\Omega\frac{dP_n}{d\Omega} , \tag{7.3}$$

where P_n is the average power radiated at frequency $\omega_n=4\pi n$ and the integration is over the two-sphere. The details of the calculation of P_n can be found in Refs. [8–10]. (Note however the following typographical errors in Ref. [8]. The term $J_{l+1}(-l\sin\phi)$ in (A.6) should be $J_{l+1}(-l\sin\theta)$ and y should be replaced by $-y$ in (A.12) and (A.13).) Because of the infinite sum appearing in (7.3), one must stop calculating the P_n numerically at some value of n, and then estimate the contribution to the sum from larger values of n. Since the sum may be slowly convergent, this "tail" may give a significant contribution even when the individual P_n are very small. For the $L=M=1$ Burden loops with $\phi\neq 0$ or π, the tail can be estimated with good accuracy because the P_n fall off as a power law $n^{-4/3}$ for large n. Durrer's results are incorrect precisely because the contribution of the tail was not included at all. In Fig. 8 we show Durrer's original results and our calculation of the sum of the first 50 terms of (7.3). Note the agreement between these values. We also show the results of the first 50 terms plus an estimate of the tail of the sum along with the results from our code. It is clear that when the tail is included, Durrer's results then agree with the results found by all other investigators. Thus, again we find that our method is in agreement with the results of previous authors.

Before continuing to compare the results of our new formulas to those in the published literature, we take a moment to discuss how piecewise linear loop trajectories are constructed to approximate smooth loop trajectories. We illustrate the procedure by explaining how the piece-

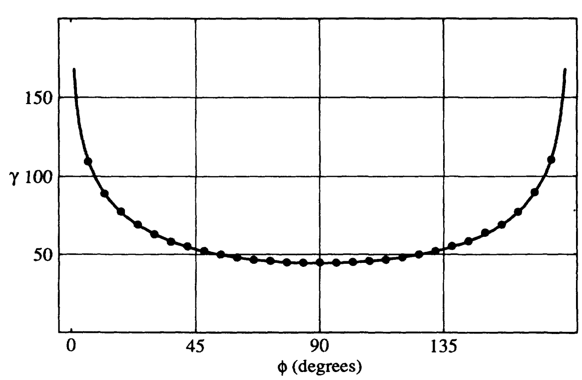

FIG. 5. The solid line is a plot of the analytic formula (7.1) for $\gamma(\phi)$ for piecewise linear trajectories in which the a and b loops are composed of just two segments each. The dots show values of γ given by our formulas for a range of angles ϕ. The agreement between the two results is so close that the dots had to be enlarged in the figure to distinguish them from the solid plot of (7.1).

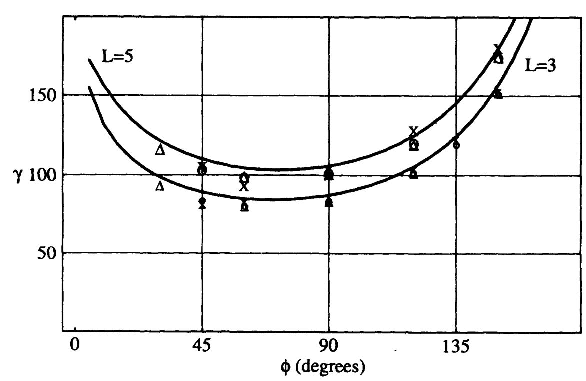

FIG. 6. The solid curves show numerical values of γ for piecewise linear loop approximations of $M=1$, $L=3,5$ Burden loops. The piecewise linear a loops were constructed to have $N_a=16L$ segments. The piecewise linear b loops each had $N_b=16M=16$ segments. The open circles show the published results of Burden [10], the crosses show the published results of Quashnock and Spergel [13], and the triangles show the results of the FFT method of Allen and Shellard [14]. We find excellent agreement among all four sets of results.

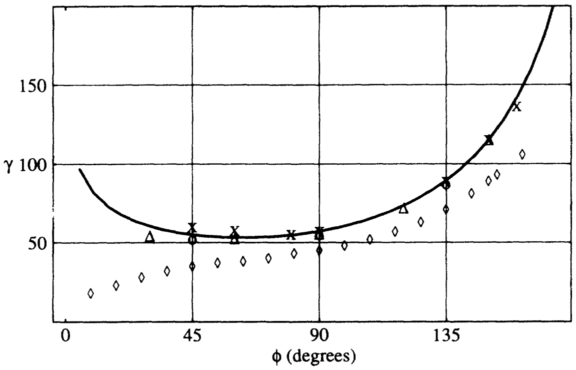

FIG. 7. Numerical values of γ for some $L=M=1$ Burden loops. The solid line shows the results of our new method. The open circles show the results of Burden, the crosses show the results of Vachaspati and Vilenkin, and the triangles show the results of the FFT method. There is excellent agreement among these four sets of results. Durrer's results are shown as open diamonds.

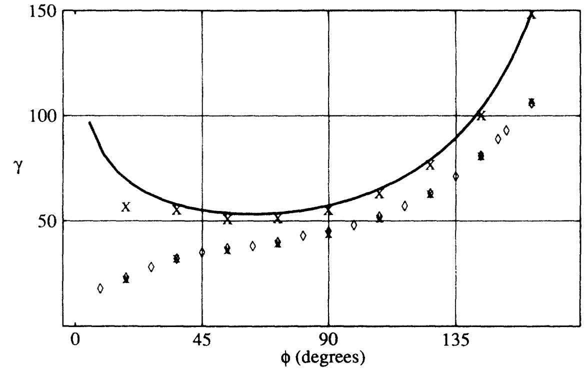

FIG. 8. The γ values reported by Durrer (open diamonds) compared to the sum of the first 50 terms (small crosses) in (7.3) for several $L=M=1$ Burden loops. Including an estimate of the contribution to γ from the infinite tail of the sum results in significantly larger values of γ (large crosses). The solid line shows the values of γ found by our formulas.

wise a and b loops were constructed to approximate the $L=M=1$ Burden loops considered above. The piecewise linear a loop was constructed by dividing the interval $u\in[0,1]$ into 16 equal segments. This defines 16 values of the coordinate u. These values were then perturbed by small random amounts so that pairs of segments on the a loop would not end up exactly parallel. [This is necessary to prevent the determinant in (4.14) from vanishing.] The perturbed values of u were then used in the first equation of (7.2) to yield the coordinates of the $N_a=16$ kinks which define the a loop. Finally, the entire a loop was translated in three space so that the kink with parameter $u=0$ was positioned at the origin. The piecewise linear b loops were constructed in a similar manner. Each b loop was constructed to have $N_b=16$ linear segments. In all cases, our values of γ were within 8% of previously calculated results with an average difference of less than 3.5%. Thus, for the purposes of calculating γ, a single wind around a smooth circular path is approximated extremely well by a set of only 16 linear segments.

We now examine how the γ values found for the piecewise linear approximation to smooth loop trajectories depends on the number of segments used. To determine this dependence we constructed several piecewise linear approximations to the $L=M=1$ Burden loops using the procedure given above, each with different values of N_a and N_b. The results of four such tests are shown in Fig. 9. One can see that the values of γ converge quickly as N_a and N_b increase. It is only for loops with values of ϕ near 0 and 180 degrees (where γ diverges) that a large number of segments are needed to obtain good accuracy. The relative errors in four approximations compared to the most accurate approximation (curve D in Fig. 9) are given in Fig. 10. The errors decrease rapidly as the number of segments increases. These errors are small and are mainly due to the loops which have ϕ close to 0 or 180 degrees. We obtained similar results for the $L=3, M=1$ and $L=5, M=1$ Burden loops. Further discussion of how the accuracy of γ in the piecewise linear approximation of a smooth loop depends on the number of segments N_a, N_b is postponed until the end of this section.

We now continue to compare the results of our formulas to those in the published literature. The next set of loop trajectories with which we compare our results is a two-parameter family of loops first studied by Vachaspati and Vilenkin [9]. The a and b loops which define these trajectories are given by

$$\begin{aligned}\mathbf{a}(u)&=\frac{1}{2\pi}[\sin(2\pi u)\hat{\mathbf{x}}-\cos(2\pi u)(\cos\phi\hat{\mathbf{y}}+\sin\phi\hat{\mathbf{z}})]\,,\\ \mathbf{b}(v)&=\frac{1}{2\pi}\left[\left[\frac{\alpha}{3}\sin(6\pi v)-(1-\alpha)\sin(2\pi v)\right]\hat{\mathbf{x}}-\left[\frac{\alpha}{3}\cos(6\pi v)+(1-\alpha)\cos(2\pi v)\right]\hat{\mathbf{y}}-[\alpha(1-\alpha)]^{1/2}\sin(4\pi v)\hat{\mathbf{z}}\right]\,,\end{aligned} \tag{7.4}$$

where α and ϕ are constant parameters, $0\le\alpha\le1$, and $-\pi<\phi\le\pi$. Note that when $\alpha=0$, these trajectories are equivalent to the $L=M=1$ Burden loops studied above. These loops have also been studied by Durrer [8]. The results found by Vachaspati and Vilenkin, and Durrer are shown in Fig. 11 along with the results of the FFT method and the results of our new method for the case $\alpha=0.5$. We find that only the FFT method and our new method are in good agreement. The γ values given by Vachaspati and Vilenkin, and Durrer appear to be too small. In fact, their results are lower than the sum of the first 300 P_n found by the FFT method (see Fig. 11). We take the sum of the first 300 P_n to be a lower bound for γ since continuing the sum to larger n or adding an estimate of the tail (or both) will only increase the value found for γ.

There are two possible explanations for the incorrect results given by Vachaspati and Vilenkin. The first possibility is that they incorrectly estimated the tail contribution to the sum in (7.3). Vachaspati and Vilenkin claim that the sum in (7.3) is rapidly convergent, with $P_n \propto n^{-3}$ for large n. However, we have found that the sum is actually much less convergent. For example, the power spectrum for the trajectory with $\alpha=0.5$ and $\phi=\pi/2$ is shown in Fig. 12. In this case, $P_n \propto n^{-1.25}$ for n in the range $100<n<300$. By overestimating the convergence of the sum in (7.3), one seriously underestimates the contribution due to the tail of the sum. The other possible explanation is that the results reported in [9] are actually for a different set of loops than those defined by (7.4). We consider this a possibility not only because the reported convergence of the sum (7.3) does not agree with our findings, but also because Vachaspati and Vilenkin include a drawing (Fig. 4 of Ref. [9]) of the loop's shape at two different times during its oscillation. However, these shapes do not agree with the shapes given by (7.4). We have confirmed that the loops shown in Fig. 4 of Ref. [9] are not the same as the loops given by (7.4), however we have been unable to resolve whether the values of γ reported in Ref. [9] correspond to the loops defined by (7.4) or to those shown in the figure [17].

We have calculated values of γ for the loop trajectories (7.4) using our new formulas for several other values of the parameter α. When $\alpha=0$, the loop trajectory is equivalent to the $L=M=1$ Burden loops. Thus, for small α, the loop trajectories (7.4) should be similar to those given by (7.2). In Fig. 13 we show our results for $\alpha=0.01$ (solid line). This is compared to results using the traditional numerical method (crosses) and the results for $\alpha=0$ (dashed line). The results of our new method agree well with those of the traditional numerical method.

The final string loop trajectories with which we compare our formulas were first given by Garfinkle and Vachaspati (Eq. (2.9) of Ref. [11]). The a and b loops for these trajectories are composed of two smooth circular arcs joined by a pair of straight segments. The analytic expressions for the a and b loops are

$$\begin{aligned}\mathbf{a}(u)&=\frac{1}{2\pi q}[\sin(\delta(u)+2\pi qu)\hat{\mathbf{x}}-\cos(\delta(u)+2\pi qu)(\cos\phi\hat{\mathbf{y}}+\sin\phi\hat{\mathbf{z}})]\ ,\\ \mathbf{b}(v)&=\frac{1}{2\pi p}[\sin(\beta(v)-2\pi pv)\hat{\mathbf{x}}-\cos(\beta(v)-2\pi pv)\hat{\mathbf{y}}]\ .\end{aligned}\tag{7.5}$$

Here, p and q are constants in the range [0,1], ϕ is the angle between the two loops, and β and δ are defined by

$$\beta(v)=(1-p)\pi[-2v] \quad\text{and}\quad \delta(u)=(1-q)\left[\frac{\pi}{2}+\pi[2u]\right]\ . \tag{7.6}$$

In (7.6), $[x]$ is the greatest integer less than or equal to x. Our results for trajectories with $(p,q)=(0.6,0.4)$, (0.4,0.8), and (0.9,0.9) are shown in Fig. 14. The results of the FFT method for several trajectories with

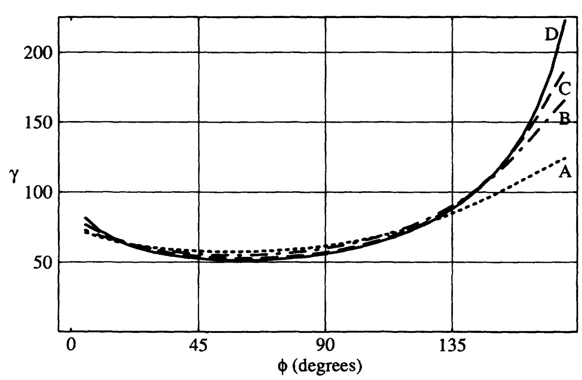

FIG. 9. Values of γ for piecewise linear approximations to the $L=M=1$ Burden loops using different numbers of segments (N_a,N_b). The number of segments (N_a,N_b) used for the curves A,B,C,D are, respectively, (6,5) (11,10), (16,15), and (36,35). The Burden loops are accurately approximated over the range $\phi\in[10,160]$ degrees when $N_a\geq 16$ and $N_b\geq 15$. Regions $\phi<10$ and $\phi>160$ when γ begins to diverge require a larger number of segments before the approximation becomes accurate.

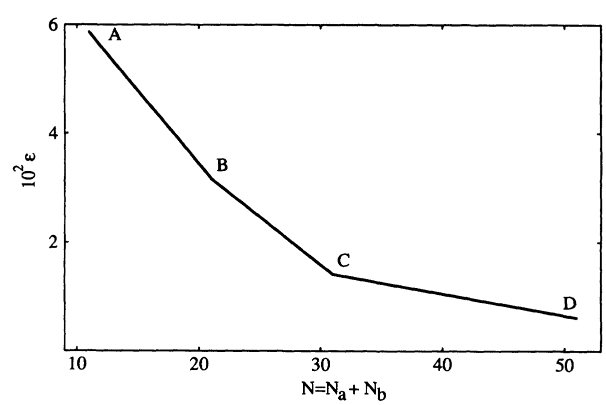

FIG. 10. Relative errors in γ for the $(N_a,N_b)=(6,5)$, (11,10), (16,15), and (26,25) piecewise linear loop approximations of the $L=M=1$ Burden loops with respect to the $(N_a,N_b)=(36,35)$ approximation. The relative error ϵ of each set of loops is calculated by summing $|(\gamma^\alpha_\phi-\gamma^E_\phi)/(\gamma^\alpha_\phi+\gamma^E_\phi)|$ over the values $\phi=5,10,\ldots,175$ degrees and then dividing by the number of terms in the sum. Here, α denotes which set of loops are being compared [i.e., $(N_a,N_b)=(6,5),(11,10)$, etc.] and E denotes the $(N_a,N_b)=(36,35)$ loops. Most of the error is due to loops with values of ϕ near 0 or 180 degrees. Increasing the number of segments from $(N_a,N_b)=(16,15)$ to (36,35) causes the average value of γ to change by less than 3%.

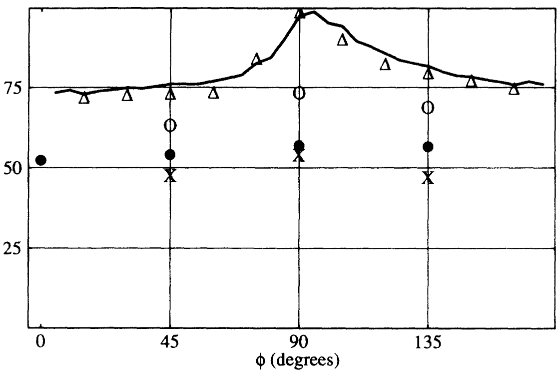

FIG. 11. Values of γ are shown for the loop trajectories given in (7.4) with $\alpha=0.5$. The results given by our formulas are shown by the solid line. The results of the FFT method are shown as triangles. There is good agreement between the FFT method and our new method. Durrer's results are shown as dots while the results of Vachaspati and Vilenkin are shown as crosses. These last two sets of results are inaccurate because the rate of convergence of the sum (7.3) was estimated incorrectly. The open circles show the sum of the first 300 terms of (7.3) as given by the FFT method. These circles should be taken as lower bounds on the values of γ.

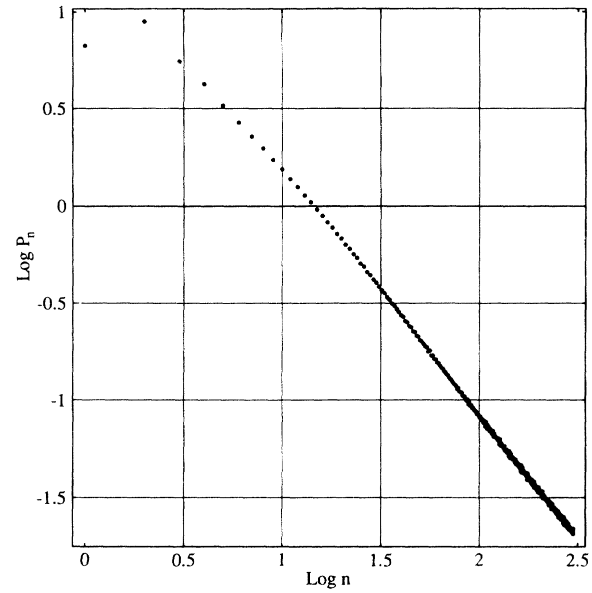

FIG. 12. The power spectrum for the trajectory (7.4) with $\alpha=0.5$ and $\phi=\pi/2$ found using the FFT method. The P_n are shown in units of $G\mu^2$. The slope of the curve for large n shows that the sum (7.3) falls off as the power law $P_n \propto n^{-1.25}$ for large n. The logarithm is to base 10.

$(p,q)=(0.9,0.9)$ are shown in Fig. 14. Again, we find good agreement between the two methods. Garfinkle and Vachaspati do not give specific values but claim that the trajectories given in (7.6) have γ values around 100. This is consistent with our results. Durrer [8] has also given values of γ for some of these trajectories. For the three trajectories with parameters $(p,q)=(0.6,0.4)$, (0.4,0.8), and (0.9,0.9) and with $\phi=\pi/2$, Durrer reports γ values of 19, 26, and 42, respectively. However, because of the errors (explained above) in other numerical results presented by Durrer, we do not have confidence in these values of γ. Durrer's results appear to be too low, which would be consistent with leaving off the contribution from the tail of the sum in (7.3). The agreement between the FFT method and our new method again gives us confidence that our formulas are correct.

We now return to the question of how accurately the γ values from piecewise linear loop trajectories approximate the γ values from smooth loop trajectories. In particular, we would like to know how the difference between the γ value of a piecewise linear loop with $N=N_a+N_b$ total segments (γ_N) and the γ value of the smooth loop that it approximates (γ_∞) falls off as a function of N. Unfortunately, we do not know how the difference $\Delta(N)\equiv|\gamma_\infty-\gamma_N|$ depends on N in the general case. However, numerical estimates may be made for individual loops with the hope that the results will hold in general. In addition, there is at least one case which has been investigated where simple analytic formulas exist for both γ_∞ and γ_N.

A detailed numerical investigation of $\Delta(N)$ has been carried out for two Burden loop trajectories (7.2) with $L=M=1$. The numerical values of γ_N have been computed over a wide range in N for both loops. The value of ϕ was arbitrarily chosen to be 39° for the first loop, and 111° for the second loop (see Fig. 15). We find that for large N, both sets of results are well approximated by functions of the form $A+BN^{-1}$, where A and B are constants that depend only upon ϕ. For the first set of results ($\phi=39°$) we find that $\gamma_N\approx 52.01+181.64N^{-1}$ for $60\le N\le 256$. By taking $\gamma_\infty=52.01$ we can find a numerical estimate of $\Delta(N)$. A similar analysis has been done for the second set of loops, where $\gamma_N\approx 64.49+97.13N^{-1}$. Figure 16 shows a log-log plot of $\Delta(N)$ for both sets of loops. By examining the slopes of the curves in Fig. 16, we find that in both cases, $\Delta(N)$ falls off like N^{-1} for large N.

In addition to the numerical investigations of $\Delta(N)$ given above, there is one case where $\Delta(N)$ has been calculated analytically. In a recent paper, Allen, Casper, and Ottewill have found a simple analytic formula for the γ values of string loops in a particular class [18]. String loops in this class have a loops which lie along a line, and b loops which lie in the plane orthogonal to that line. In particular, when the b loop takes the shape of an N_b-sided regular polygon, γ_{N_b} is given by

$$\gamma_{N_b}=32\left[1-\cos\left[\frac{2\pi}{N_b}\right]\right]\left[\frac{1}{2}N_b\ln N_b+\sum_{j=2}^{N_b-1} j\ln(j)\cos\left[\frac{2\pi}{N_b}j\right]\right]. \tag{7.7}$$

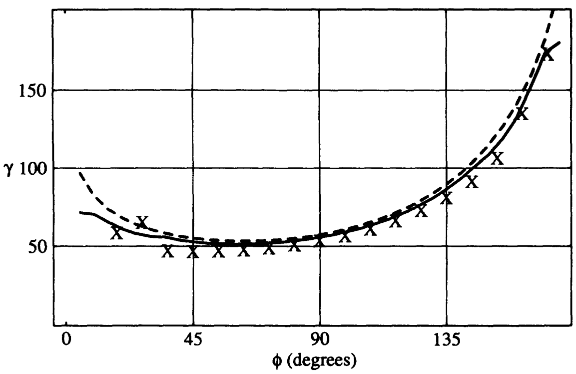

FIG. 13. Values of γ are compared for the loop trajectories given in (7.4) with $\alpha=0.01$. The results of our formulas are shown by the solid line. The results of the traditional numerical method are shown as crosses. The two methods are in good agreement. The values of γ when $\alpha=0$ are shown by the dashed line.

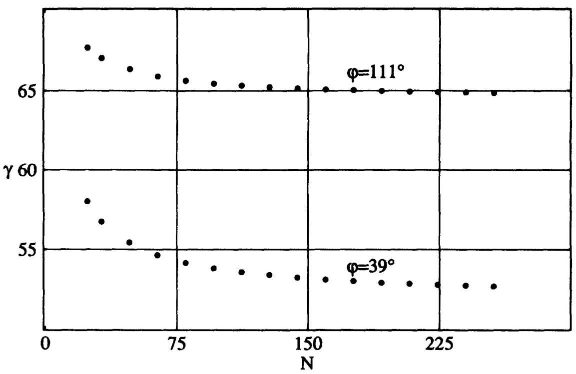

FIG. 15. The γ values from a series of increasingly accurate piecewise linear loop approximations to two $(L=M=1)$ Burden loops. The total number of linear segments in each approximation is given by N. Both sets of γ values quickly converge to their asymptotic limits.

When the b loop takes the shape of a perfect circle, γ is found to be

$$\gamma=16\int_0^{2\pi}dx\frac{1-\cos x}{x}\approx 39.002\,454\ . \tag{7.8}$$

Since an N_b-sided polygon becomes a perfect circle in the limit as N_b goes to infinity, the difference between Eqs. (7.7) and (7.8) give $\Delta(N_b)$. Figure 7 of Ref. [18] shows a log-log plot of $\Delta(N_b)$. From this plot one finds that, in this case, $\Delta(N_b)$ falls off as N_b^{-2}. The reason that the γ values from the piecewise linear loops converge to the smooth loop limit faster in this case than in the previous cases is most likely because the a loop in this case is already piecewise linear. While we do not know how the errors in γ_N scale with increasing N in the general case, it seems reasonable to conjecture that the errors fall off as N^{-1} for large N.

As a point of interest, it takes only 14 sec to calculate γ for a loop with $N=N_a+N_b=32$ on a Sun-4 workstation (SS2). The calculation time for γ scales roughly as N^4. The speed of this algorithm makes it feasible to calculate γ for loops with large numbers of segments N_a and N_b. It is also possible to rapidly calculate γ for very large numbers of loops with moderate values of N_a and N_b.

In this section we have shown that in all cases where previously published numerical methods have given reliable results for γ, these results are in good agreement with those given by our exact formulas. The large number of both piecewise linear and smooth loop trajectories for which our formulas have confirmed previously published results gives us confidence that our method is

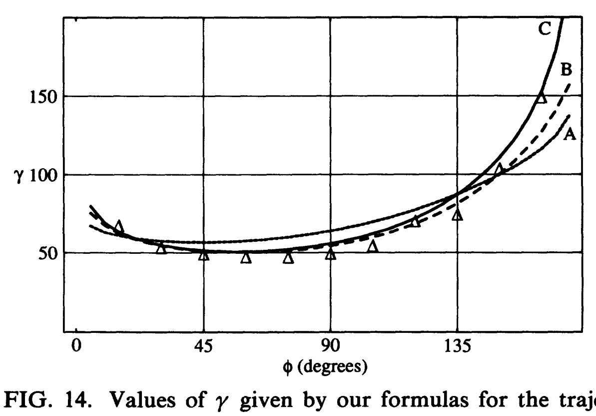

FIG. 14. Values of γ given by our formulas for the trajectories (7.5) for three sets of parameters (p,q) and a range of angles ϕ. Curves A, B, and C give the results for trajectories with $(p,q)=(0.6,0.4)$, $(0.4,0.8)$, and $(0.9,0.9)$, respectively. These results are consistent with the claim by Garfinkle and Vachaspati that the trajectories (7.5) have γ values on the order of 100. The results of the FFT method with $(p,q)=(0.9,0.9)$ are shown by the triangles, and should be compared to curve "C." There is good agreement between the two methods.

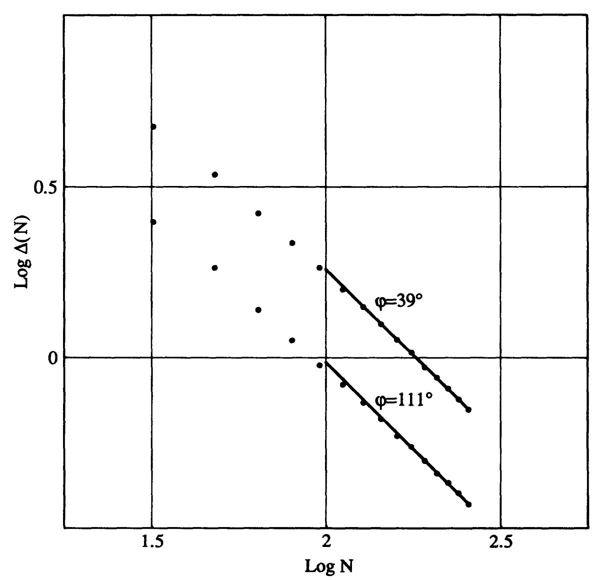

FIG. 16. The function $\Delta(N)$ for two $(L=M=1)$ Burden loops. Each point shows the difference between the γ value for a piecewise linear approximation with N segments and the numerical estimate of γ in the $N=\infty$ limit. Both of the solid lines have a slope of -1, showing that the errors fall off as N^{-1}. The logarithm is to base 10.

correct. In cases where our method yields results that disagree with previously published results, we have shown that our results are correct. We have shown this by identifying the errors in the previously published work and by showing that our results are consistent with those given by other independent methods such as the FFT method of Allen and Shellard [14] and/or a corrected implementation of the numerical method used by the original author(s). Since our results have been correct for every trajectory tested so far, we have confidence that our formulas provide a reliable method for calculating the power radiated in gravitational waves for arbitrary cosmic string loops.

VIII. CATALOG OF LOOPS

This section gives a short catalog of piecewise linear loop trajectories and their γ values. This catalog is intended to give a number of simple cases which might prove useful in testing future analytic or numerical methods. The a and b loops which define these trajectories are regular polygons formed with small numbers of segments N_a and N_b. With each pair of a and b loops we form a two parameter family of loop trajectories. The two parameters (ϕ and θ) describe the relative orientation of the a and b loops. There is nothing special about these loops other than that they are simple piecewise linear trajectories.

The first set of trajectories we consider are defined by a and b loops consisting of two and three segments, respectively. The three segment b loop has the shape of an equilateral triangle. (The simplest case, where the a and b loops each have just two segments is discussed in the previous section.) The a loop is taken to lie along the z axis. One kink on the a loop is positioned at the origin; the parameter $u=0$ at this kink. The other kink (at $u=\frac{1}{2}$) is positioned above the first kink and has coordinates $(0,0,\frac{1}{2})$. For the b loop we again position one kink at the origin and set the parameter $v=0$ at that kink. The position of the other two kinks depends on the parameters ϕ and θ. When $\phi=\theta=0$, the b loop lies in the $x-z$ plane. The kink at $v=\frac{1}{3}$ has coordinates $(-\frac{1}{6},0,\sqrt{3}/6)$ and the kink at $v=\frac{2}{3}$ has coordinates $(\frac{1}{6},0,\sqrt{3}/6)$. When ϕ and θ are not zero, the position of the b loop is found as follows. First, the b loop is rotated by the angle $\phi>0$ about the z axis (counterclockwise when viewed from large positive z). After the ϕ rotation, the b loop is then rotated by the angle $\theta>0$ about the x axis (counterclockwise when viewed from large positive x). Values of γ for the trajectories defined by these a and b loops are given in Table I for several values of the angles ϕ and θ. In generating Table I, we have been careful to avoid certain values of ϕ and θ for which the a and b loops have special relative positions. In particular, if the a and b loops are exactly coplaner, the operator D becomes singular. In this case, accurate values of γ may still be found by examining trajectories where the angles ϕ and θ deviate very slightly from their desired values. However, since the γ values given in this section are meant to be "benchmark" values for future work, we have not included such cases here. In the following tables, certain pairs of angles are omitted for similar reasons.

TABLE I. Values of γ for the first set of trajectories for several values of the angles ϕ and θ.

$\theta\backslash\phi$	0°	18°	36°	54°	72°
18°	59.33	59.80	61.21	63.51	66.30
36°	53.81	54.56	56.86	60.93	67.45
54°	49.35	50.15	52.56	56.40	60.72
72°	46.70	47.54	50.12	54.47	60.36
90°	45.83	46.70	49.37	54.12	62.25

TABLE II. Values of γ for the second set of trajectories.

$\theta\backslash\phi$	18°	36°	54°	72°	90°
18°	100.85	90.65	74.48	64.80	58.92
36°	82.00	76.01	70.97	64.82	59.98
54°	72.61	66.51	63.68	61.54	59.95
72°	67.04	61.24	59.12	58.80	60.02
90°	63.97	58.53	56.80	57.12	59.75

The second set of trajectories we consider are defined by a and b loops consisting of three segments each. Both the a and b loops are equilateral triangles. The position of the b loop depends on the two parameters ϕ and θ in exactly the same way as the b loop in the first set of trajectories. The a loop is placed in the same position the b loop has for parameter values $\phi=\theta=0$. Values of γ for the trajectories defined by these a and b loops are given in Table II for several values of the angles ϕ and θ.

The third set of trajectories we consider are defined by a and b loops consisting of two and five segments, respectively. The two segment a loop is identical to the a loop used in the first set of trajectories. The b loop is taken to be a pentagon. One kink on the pentagon is positioned at the origin and is chosen to have parameter value $v=0$. When $\phi=\theta=0$, the b loop lies in the x-z plane, and is positioned so that the kink at $v=\frac{1}{5}$ has coordinates $[-\frac{1}{5}\cos(\pi/5),0,\frac{1}{5}\sin(\pi/5)]$, the kink at $v=\frac{2}{5}$ has coordinates

$$(\tfrac{1}{5}[\sin(\pi/10)-\cos(\pi/5)],0,\tfrac{1}{5}[\cos(\pi/10)+\sin(\pi/5)]) ,$$

and so on. When ϕ and θ are not equal to zero, the b loop is rotated in exactly the same manner as for the previous two sets of loop trajectories. Values of γ for the trajectories defined by these a and b loops are given in Table III for several values of the angles ϕ and θ.

The fourth set of trajectories we consider are defined by a and b loops consisting of five and three segments, re-

TABLE III. Values of γ for the third set of trajectories.

$\theta\backslash\phi$	0°	18°	36°	54°	72°
18°	63.52	64.15	66.04	69.28	74.52
36°	54.07	54.99	57.78	62.31	67.63
54°	47.69	48.74	52.02	57.78	66.36
72°	44.20	45.30	48.74	54.98	64.04
90°	43.10	44.20	47.69	54.08	63.95

TABLE IV. Values of γ for the fourth set of trajectories.

$\theta \backslash \phi$	18°	36°	54°	72°
18°	84.69	75.43	67.82	62.44
36°	77.37	71.03	65.71	61.86
54°	70.11	65.69	62.72	60.42
72°	64.41	61.37	61.13	61.33
90°	60.49	58.21	60.49	—

TABLE V. Values of γ for the fifth set of trajectories.

$\theta \backslash \phi$	18°	36°	54°	72°
18°	114.46	94.04	80.22	68.84
36°	93.52	82.49	72.06	65.40
54°	77.15	72.94	67.22	62.74
72°	67.11	64.76	64.05	62.98
90°	61.24	59.47	61.24	—

spectively. The a loop is a pentagon placed in the same position as the b loop in the third trajectory set for parameter values $\phi=\theta=0$. The b loop is an equilateral triangle whose position is given in terms of the parameters ϕ and θ in exactly the same way as the b loops used in the first and second trajectory sets. Values of γ for the trajectories defined by these a and b loops are given in Table IV for several values of the angles ϕ and θ.

The final set of trajectories we consider are defined by a and b loops consisting of five segments each. Both loops are taken to be pentagons. The a loop is identical to the a-loop used in the fourth set of trajectories. The b loop is in the same position as the a loop when $\phi=\theta=0$. When ϕ and θ are not zero, the b loop is rotated in the same manner as in the previous sets of trajectories. Values of γ for the trajectories defined by these a and b loops are given in Table V for several values of the angles ϕ and θ.

The five sets of loop trajectories along with the γ values given in this section are intended as "benchmark values" for future analytic or numerical work.

IX. CONCLUSION

We have derived a new method for calculating the power emitted in gravitational radiation by cosmic string loops. This method yields an *exact analytic formula* in the case of piecewise linear cosmic string loops. By increasing the number of segments used, piecewise linear string loops can approximate any cosmic string loop *arbitrarily closely.* Our formula (derived in Secs. V and VI) involves nothing more complicated than logarithmic and arctangent functions. No numerical integrations are required. Further, since our formula is exact, there is no need to estimate any contribution to γ from the "tail" of an infinite sum. The error introduced when approximating smooth loop trajectories by piecewise linear trajectories has been investigated. It is found that this error typically falls off as N^{-1} for large N, although in at least some cases it falls of faster, as N^{-2}. We believe that for "generic" loops the error scales as N^{-1}. Using a computer to evaluate the approximately N^4 terms in our formula, we can determine values of γ more accurately and more efficiently than by previously published methods.

We have tested the results of our formula against all previously published radiation rates for different loop trajectories. Section VII contains a detailed comparison of the results given by our new method to those reported by previous authors. In every case, our formula is found to give the correct result. In many cases our results are in good agreement with the published data. However there are also a number of cases where our results do not agree with those previously published. There are, in fact, a number of cases where conflicting results have been published for the same trajectories. In the cases where a disagreement was found we have identified the errors made in the published work which led to the incorrect results. In most cases, the errors in the published values of γ are a result of underestimating the contribution of the tail of the infinite sum in (7.3). The incorrect values of γ which have been published are typically 25–50% below the correct results. We are confident that our formula gives the correct results because, in every case, we have shown our results to be consistent with those given by independent methods.

We intend to use this exact formula in future work, for example to repeat some of the work of Scherrer, Quashnock, Spergel, and Press [12] concerning the distribution of γ values of non-self-intersecting loops. In addition, we plan to show how this formula may be modified to yield similar analytic results for the linear momentum radiated by cosmic string loops [17].

ACKNOWLEDGMENTS

This work was supported in part by NSF Grant No. PHY-91-05935 and a NATO Collaborative Research Grant. The work of P.C. was also supported in part by Department of Education Grant No. 144-BH22. We would like to thank C. Burden, R. Durrer, and T. Vachaspati for useful correspondence concerning their work. We are particularly grateful to Adrian Ottewill for a number of useful conversations concerning this work, including the tests in (6.5) and (6.6), the definition of the operator D, and for providing an independent test of the formulas.

[1] T. W. B. Kibble, J. Phys. A **9**, 1387 (1976); T. W. B. Kibble, G. Lazarides, and Q. Shafi, Phys. Rev. D **26**, 435 (1982).

[2] Y. B. Zel'dovich, Mon. Not. R. Astron. Soc. **192**, 663 (1980).

[3] A. Vilenkin, Phys. Rev. D **24**, 2082 (1981); A. Vilenkin, Phys. Rep. **121**, 263 (1985).

[4] A. Albrecht and N. Turok, Phys. Rev. Lett. **54**, 1868 (1985); Phys. Rev. D **40**, 973 (1989); A. Albrecht, in *The Formation and Evolution of Cosmic Strings,* Proceedings of

the Symposium, Cambridge, England, 1989, edited by G. W. Gibbons, S. W. Hawking, and T. Vachaspati (Cambridge University Press, Cambridge, England, 1989).

[5] D. Bennett and F. Bouchet, Phys. Rev. Lett. **60**, 257 (1988); **63**, 2776 (1989); Astrophys. J. **354**, L41 (1990); in *The Formation and Evolution of Cosmic Strings* [4]; Phys. Rev. D **41**, 2408 (1990).

[6] B. Allen and E. P. S. Shellard, Phys. Rev. Lett. **64**, 119 (1990); E. P. S. Shellard and B. Allen, in *The Formation and Evolution of Cosmic Strings* [4].

[7] R. R. Caldwell and B. Allen, Phys. Rev. D **45**, 3447 (1992).

[8] R. Durrer, Nucl. Phys. **B328**, 238 (1989).

[9] T. Vachaspati and A. Vilenkin, Phys. Rev. D **31**, 1052 (1985).

[10] C. Burden, Phys. Lett. **164B**, 277 (1985).

[11] D. Garfinkle and T. Vachaspati, Phys. Rev. D **36**, 2229 (1987).

[12] R. J. Scherrer, J. M. Quashnock, D. N. Spergel, and W. H. Press, Phys. Rev. D **42**, 1908 (1990).

[13] J. M. Quashnock and D. N. Spergel, Phys. Rev. D **42**, 2505 (1990).

[14] B. Allen and E. P. S. Shellard, Phys. Rev. D **45**, 1898 (1992).

[15] S. Weinberg, *Gravitation and Cosmology* (Wiley, New York, 1972), Eq. 10.4.13.

[16] J. D. Jackson, *Classical Electrodynamics* (Wiley, New York, 1975), Eq. 12.133.

[17] T. Vachaspati (private communication).

[18] B. Allen, P. Casper, and A. Ottewill, Phys. Rev. D (to be published).

[19] B. Allen, P. Casper, and A. Ottewill, "Closed Form expression for the Momentum Radiated from Cosmic String Loops," Report No. WISC-MILW-94-TH-15, 1994 (unpublished).

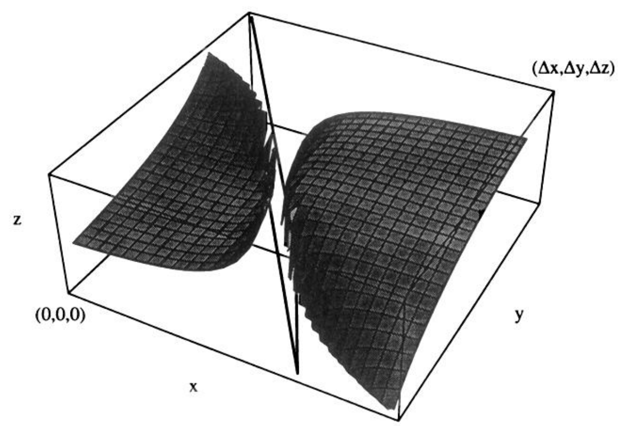

FIG. 2. The delta function $\delta[f(x,y,z)]$ which appears in (5.2) only has support when $f(x,y,z)=0$. Solving $f(x,y,z)=0$ for $z(x,y)$ we find that the surface $z(x,y)$ consists of a pair of disconnected hyperbolic sheets. The hyperbolic sheets are separated by the plane $\beta_1 x + \beta_2 y + \beta_4 = 0$, where the denominator of (6.4) vanishes. The intersection of a $z=$const plane with these sheets will be a hyperbola in the x-y plane. The integration volume for (5.2) is a box with opposite corners (0,0,0) and $(\Delta x, \Delta y, \Delta z)$.